The mixed state in superconducting microstructures

A. N. Lykov

P. N. Lebedev Physics Institute, Russian Academy of Sciences, Moscow

(Submitted 11 March 1992; resubmitted after revision 2 June 1992)
Usp. Fiz. Nauk **162**, 1–62 (October 1992)

This paper presents a review of investigations of the mixed state in artificial microstructures based on type II superconductors. It discusses bridge contacts of dimensions which are large compared to the coherence length, as well as planar multielement structures and layered superconducting structures. The present state of this field and the short-range prospects for its development are analyzed.

INTRODUCTION

The investigation of the mixed state in artificially prepared superconducting microstructures is a problem of present importance. This field of research unites two apparently distant areas of superconductivity: microelectronics and high-current superconductivity. There are three aspects that contribute to the great interest in this field. First, by creating superconducting microstructures one can tailor the properties of a material in a manner that would not be possible by other means. Second, these structures provide additional possibilities both for determining the interaction of an individual vortex with an inhomogeneity (elementary pinning), and for finding the bulk pinning force (the procedure for summing these elementary forces). This direction of research is important because the maximum critical current I_c that can flow in type II superconductors without energy dissipation is governed by the ability of the defects to prevent the motion of (pin) the vortex lattice. The theoretical calculation of the bulk pinning force is in general a complicated problem. In the absence of a unique general theory there exists a host of theoretical approaches for solving specific problems. In this sense, the study of the mixed state in superconducting microbridges is agreeably different: these investigations can be carried out by a single approach based on the Ginsburg–Landau theory.[1] Third, the variety of vortex microbridges is interesting from the point of view of microelectronics, since the ordered coherent motion of the vortices generates electromagnetic radiation. The importance of this area of research has not been diminished since the discovery of the oxide-based high-temperature (high-T_c) superconductors, which, as has been shown, are type II superconductors with a short coherence length $\xi(0) \sim 10$ Å (Ref. 2).

In order of their significance, one can distinguish three kinds of artificial superconducting microstructures: bridge contacts, planar multielement structures, and layered superconducting structures. This review presents an analysis of the properties of these devices. It will touch very little on the properties of Josephson junctions. In the past decade this topic has received a great deal of attention, and some excellent monographs have been published, e.g., Refs. 3 and 4.

1. VORTEX MICROBRIDGES

1.1. A brief classification of microbridges

The processes occurring in bridge junctions are determined largely by the following parameters: the characteristic dimensions of the bridge, and, depending on the temperature, the coherence length $\xi(T)$ and the mean free path l of the electrons in the bridge. Among the characteristic dimensions is the so-called effective length of the microbridge. It is necessary to introduce this quantity because for a finite voltage across the bridge the modulus of the order parameters, which characterizes the superconducting state, changes, not only in the microbridge itself, but also in a certain region around it. This parameter has the meaning of the distance along the microbridge in which this process is localized. The most interesting case from the applied point of view and for simplicity of analysis is that where the characteristic dimensions of the bridge are small compared to $\xi(T)$ and to $\lambda(T)$, the penetration of the field in the superconductor, but large compared to $\min[l,(\xi_0 l)^{0.5}]$, where ξ_0 is the range of action of the kernel in the equation of self-consistency for determining the energy gap in the spectrum of excitations in a clean superconductor, and moreover, when the temperature is near the critical temperature of the "banks" of the bridge. This circumstance allows us to use in the analysis of the processes in the bridges the Ginsburg–Landau equations, to which the more complicated equations of the microscopic theory of superconductivity reduce in this case. The equations for the order parameter ψ at distances from the contact much less than $\xi(T)$ and for a superconducting current density j_s are[5]

$$\nabla^2\psi = 0, \tag{1.1a}$$

$$j_s \sim \mathrm{Im}(\psi^* \nabla\psi), \tag{1.1b}$$

where ∇^2 is the Laplacian. As a result, the behavior of the bridge contacts is described by at most two equations for the current I and the voltage V (Refs. 4, 5)

$$I = I_c \sin\varphi + (V/R), \tag{1.2a}$$

$$V = (\hbar/2e)\,\partial\varphi/\partial t, \tag{1.2b}$$

 0038-5670/92/100811-31$03.00

where R is the resistance of the contact in the normal state, I_c is the critical current of the contact, t is the time, φ is the phase difference of the order parameter, and $\hbar$ is Planck's constant. Equation (1.2a) represents the current flowing through the contact as a sum of the superconducting component, $I_c \sin \varphi$ and the ordinary normal component V/R. Despite its simplicity, the resistive model gives a good qualitative, and in some cases quantitative, description of the effects that are of the greatest interest from the point of view of applications observed in various Josephson structures. This is why this model is so widely used. For example, the dc Josephson effect arises when the current through the junction is less than the critical current, $I < I_c$. Then the phase difference is such that $I_s = I$ and there is no voltage across the junction. If a weak link is created not by a superconductor (but by a dielectron, for example), this result is not *a priori* obvious. A magnetic field penetrating into the Josephson junction of a superconducting loop containing such a junction attenuates the superconducting current, and it is thereby possible to use this effect for making sensitive devices. If $V \neq 0$, then φ increases and the superconducting current I_s varies in time (oscillates with the frequency $2eV/\hbar$ even if V is a constant. This is the so-called ac Josephson effect. The coefficient of proportionality between the applied voltage and the oscillation frequency is 483.6 mHz/μV. One of the manifestations of the ac Josephson effect is the appearance of current steps on the current-voltage (I–V) characteristics of the contacts, when they are placed in an external magnetic field. The positions of these steps are given by

$$V_n = n\hbar\omega/2e, \tag{1.3}$$

where n is the number of the current step and ω is the frequency of the radiation. This effect can easily be explained by the resistive model if only a single term $I_\omega \sin \omega t$ is retained on the right-hand side of Eq. (1.2a), where I_ω is the amplitude of the ac current induced in the contact by the external radiation.

In addition, the actual properties of Josephson junctions with direct conductivity, which includes short bridge contacts, are much more complicated than the resistive model implies. This comment applies particularly to transient processes. A number of effects are observed on these contacts that cannot be explained by that model. Among the most interesting effects of this sort are a frequency dependence of the amplitude of the superconducting current, the induction of supeconductivity by external electromagnetic radiation, the existence of excess current, and a series of features on the I–V characteristic, located according to the relation $V_n = 2\Delta/ne$, where Δ is the gap in the spectrum of elementary excitations and n is an integer. A theoretical analysis of these effects is difficult because the simplified non-steady-state Ginsburg–Landau equations, on which the resistive model is based, are valid only for gapless superconductors. In spite of these difficulties, a definite degree of success has been obtained in understanding the processes in these contacts. For example, Aslamazov and Larkin[6] have shown that a high-frequency electromagnetic field can cause effective cooling of the electrons at the contact, which also leads to an increase in the critical current of the contacts in a microwave field. In the work reported in Refs. 7 and 8 a microscopic theory was used to calculate the I–V characteristics of a short microbridge. It was shown that for high voltages

$$I(V) \approx \frac{V}{R} + \frac{\Delta}{\mathrm{Re}[(\pi^2/4) - 1]},$$

whereas in the resistive model this characteristic quickly becomes ohmic. An interesting mechanism for the appearance of a gap structure in the I–V characteristics, based on multiple Andreev reflections of quasiparticles at the boundaries of the microbridge, has been proposed in Refs. 9 and 10.

Bridges with a length $l_m \gg \xi(T)$, $\lambda(T)$, and with a width w and thickness d smaller than those last two quantities, are narrow superconducting channels. It is well known[11] that in such structures the generation of a voltage is associated with phase-slip centers. Since the width and thickness of the bride is less than the penetration depth of the magnetic field, the current is distributed uniformly over the transverse cross section, and in the region of applicability of the Ginsburg-Landau theory the critical current is given by the depairing current

$$j_c = \frac{cH_c(T)}{3\sqrt{6\pi}\,\lambda(T)}, \tag{1.4}$$

where $H_c(T)$ is the thermodynamic critical magnetic field and c is the velocity of light. Skocpol[12] has observed good agreement between the experimentally determined critical current density and the current density given by this formula. If the transport current is greater than I_c, then the filament goes over into the resistive state. Unlike the situation in short bridges, in long bridges it is difficult to observe coherent effects resembling the Josephson effect. Ordinarily such effects arise in connection with the presence of "weak spots' in the sample—small inhomogeneities at the sample edges.

Processes of another kind are seen in short but wide bridges, where $l_m \ll \xi(T)$ and $w > \xi(T)$. The main effects characteristic of Josephson junctions, such as the current steps produced by an electromagnetic field in the I–V characteristics at voltages given by relation (1.3), can be observed in these bridges. This was shown to be the case first by Anderson and Dayem,[13] and their conclusions were confirmed in a number of studies, e.g., Ref. 14. In these experiments the measurements were carried out on thin-film contacts with a constriction a few microns in width. The bridges were prepared by vacuum deposition through a mask. Examples of the I–V characteristics measured in Ref. 13 are shown in Fig. 1.

For bridges of variable thickness the boundaries of the formation of Abrikosov vortices were found in superconducting bridges of various dimensions.[15,16] In these papers it was proposed that the effective widths of the bridges coincide with l_m, i.e., the nonlinear processes are localized at the contacts. In bridges of variable thickness this is made possible by their small thickness as compared to the thickness of the "banks." The calculations were carried out for temperatures near T_c on the basis of the Ginzburg–Landau equations. Figure 2 shows a diagram of the possible states derived in these investigations. As the length of a wide microbridge increases there is a transition at $l_m = 3.49\,\xi(t)$ in a bridge of variable thickness from the formation of Josephson vortices,

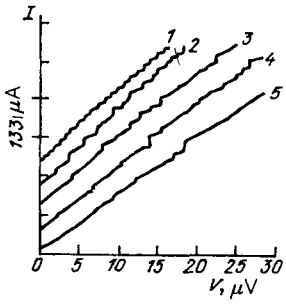

FIG. 1. I–V characteristics of a contact based on a tin film in a microwave field of frequency (in GHz) *1*) 0.28; *2*) 0.94; *3*) 3.8; *4*) 6.8; and *5*) 9.35. Scale on the current axis is 133 μA (Ref. 13).

which do not contain a non-superconducting core, to the formation of ordinary Abrikosov vortices. The experimental limit determined in Ref. 18 for tin microbridges of variable thickness proves to be close to the theoretical value. This limit was found from the deviation between the behavior of microbridges in a microwave field as implied by the resistive model, and the Josephson behavior as the temperature was lowered and thus the temperature-dependent coherence length was varied. Contacts with constriction dimensions greater than the effective penetration depth of a magnetic field ($\lambda_\perp = \lambda^2/d$) in thin superconducting films are similar in their properties to ordinary superconducting films.

1.2. Vortex microbridges formed of ordinary low-temperature superconductors

The properties of the contacts are quite different for constrictions of different dimensions. In microbridges that are small compared to coherence lengths the normal and superconducting components of the current are distributed uniformly over the entire contact. In bridges with large dimensions the Josephson effects are due to the periodic motion of the quantized vortices in the narrowest part of the contact, that is, in this case the simple dependence between the current and the phase difference can no longer be obtained. The formation of current steps in the I–V characteristics of these microbridges is due to the synchronization of the motion of the vortices by an external electromagnetic field. In large bridges it is not possible to refer to the Josephson effect in a strict sense, since in the region of the contact not only the phase, but also the amplitude of the order parameter changes. In the experiments of Anderson and Dayem[13] the formation of steps on the I–V characteristics was extremely sensitive to an external magnetic field. Sometimes the step structure on the characteristics disappeared even in a magnetic field of ~0.1 G. This effect happens because even a small magnetic field can allow the vortices to penetrate into the film and into microbridges made from the film, and the additional vortices there can greatly hinder the synchronization of their motion. At the same time, there are papers, e.g. Ref. 19, where the step structure on the I–V characteristics was observed in very strong magnetic fields ($\gtrsim 1$ kG). The measurements were made on bridges with large dimensions (up to 20 μm long), prepared from tin or lead films by means of pulsed electrical breakdown. Moreover, in this paper the experimenters observed an increase in the voltage spacing between the current steps when the magnetic field on the microbridge was increased.

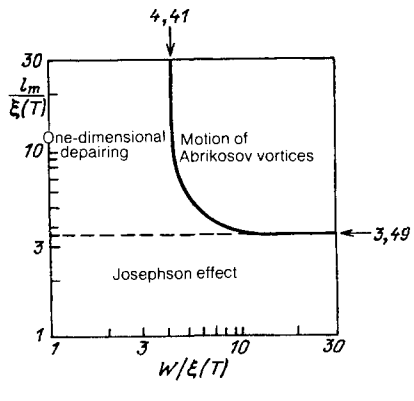

FIG. 2. Possible dimensions of microbridge contacts (Ref. 16).

Films of Sn or In are most frequently used to study the properties of bridge contacts. Films of these superconductors are very easy to prepare by vacuum deposition, and their superconducting transition temperatures are close to those obtained for bulk samples. The difficulties in working with these materials are due to the formation of whiskers and hairline cracks during thermal cycling from room temperature to the temperature of liquid helium. During cooling the metal contracts more than the substrate, and therefore the film is inelastically elongated. Upon being heated to room temperature the film then is compressed. The formation of stresses leads to degradation of the sample. Films of the refractory metals Nb, V, and Ta are less susceptible to degradation, which to a large measure explains the heightened interest in investigations of microbridges based on those metals.[20–22] However, in these superconductors the coherence length is considerably less than in tin and indium. For niobium, for instance, $\xi_0 = 350$–400 Å. Because of these short coherent lengths, it is extremely difficult to make a microbridge with constriction dimensions less than the coherence length.

It is well known[4] that bridges with large dimensions are not as good as bridges with small ones or other Josephson contacts from the point of view of their use in a variety of electronic devices. Nonetheless, the use of these bridges is of considerable interest. In addition to the observation of effects similar to the Josephson effect in these contacts, they are of interest because their properties are determined by the behavior of a small number of vortices. This facilitates the theoretical analysis of their properties. Moreover, in the case of wide bridges the effective penetration depth of a magnetic field, which determines the size of the electromagnetic region of a vortex, is ordinarily greater than the dimensions of the bridge. For low voltages, where the interaction between the vortices is small, it is possible to have them move in a single row. This case has been analyzed in Refs. 23 and 24. Aslamazov and Larkin[24] have studied a contact made up of a superconducting film of thickness d with two cuts along a common straight line, where the distance between the ends of the cuts is $w \ll \lambda_\perp$ (Fig. 3). It was shown in this paper that the principal results do not depend on the shape of the contact, which has a strong influence only on the critical current I_c. For a superconducting current density j_s in the region of

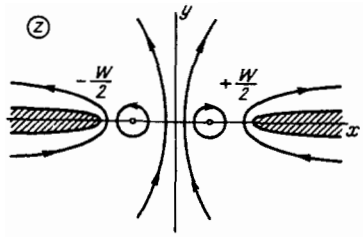

FIG. 3. Superconducting contact with two quantized vortices (Ref. 24).

the contact where it is less than the critical current density the following expression was used in Ref. 24:

$$\mathbf{j} = \frac{c^2\hbar}{8\pi e\lambda^2}\nabla\varphi. \tag{1.5}$$

The equation for the phase φ of the order parameter is obtained from the condition div $\mathbf{j} = 0$ and has the form

$$\nabla^2\varphi = 0 \tag{1.6}$$

with the boundary condition $\partial\varphi/\partial\mathbf{n} = 0$ (here $\mathbf{n}$ is the normal to the surface of the superconductor). Solving the Laplace equation Eq. (1.6), one can find the phase distribution, the current density in the region of the contact, and the forces acting in this region on the vortices.

The current lines are hyperbolae with foci at the points $x = \pm w/2$. The x axis, as shown in Fig. 3, lies in the plane of the film and lies crosswise to the bridge, with the origin at the center of the bridge. The current density j on the x axis in the region of the contact is

$$j = \frac{I}{\pi d\,[(w/2)^2 - x^2]^{1/2}}. \tag{1.7}$$

For a vortex on the x axis on the edge of the contact at a point close to $w/2$, the force on it is

$$F_n = \frac{\hbar}{2e}I_0\Big[\frac{2}{w-2x_n} - 2q_n\frac{I}{I_0[w(w-2x_n)]^{1/2}} + \frac{2}{[w(w-2x_n)]^{1/2}}\sum_{n\neq m}q_nq_m\left(\frac{w+2x_m}{w-2x_m}\right)^{1/2}\Big], \tag{1.8}$$

where x_m are the coordinates of the rest of the vortices that also are located on the x axis, $I_0 = c^2\hbar d/8e\lambda^2$ and is of the order of magnitude of the critical current of a contact with a dimension $\sim\xi$, and $q_n = \pm 1$, depending for each vortex on its direction. It follows from Eq. (1.8) that the force of attraction of the vortex towards the edge of the contact (the first term) increases with its approach to the edge faster than the force of interaction with the current (the second term). Therefore, for small currents there is an energy barrier that prevents the vortex from entering the contact. The barrier for the formation of the first vortex vanishes at the critical current I_c, which is determined from the conditions of equality of these forces at $x-(w/2)\sim\xi$. From this we obtain $I_c = I_0(w/\xi)^{1/2}$. Near the critical temperature it varies as $(T_c - T)^{1.25}$.

If the contact already contains vortices, then the barrier to the formation of new vortices is changed. From formula (1.8) it follows that in this case the barrier vanishes at a current $I = I_c + \Delta I$, where ΔI is

$$\Delta I = I_0\sum_m q_m\left(\frac{w-2x_m}{w+2x_m}\right)^{1/2}. \tag{1.9}$$

A vortex formed at the edge must move to the center of the contact. As can be seen from formula (1.8), at a distance greater than ξ from the edge the force of attraction to the edge is less than the force of interaction with the current. Furthermore, the ratio of the force acting on the vortex from the other vortices [the third term in formula (1.8)] to the force of interaction of the vortex with the current is of the order of magnitude $\Delta I/I$. For small voltages across the contact, where $\Delta I \ll I$, the motion of the vortices occurs mainly as a result of the force of interaction of the vortex with the transport current. To find the form of the I–V characteristics, Benacka *et al.*[19] used the usual equation of viscous motion of a vortex

$$\eta\partial x_n/\partial t = F_n, \tag{1.10}$$

where η is the coefficient of viscosity, for which there exists an expression in terms of the microscopic parameters of the superconductor,[25] and F_n is the force of interaction of the vortex with the current. The latter is given by the expression

$$F_n = -\frac{2\hbar I q_n}{e(w^2 - 4x_n^2)^{1/2}}, \tag{1.11}$$

i.e., as seen from formula (1.7), this force is proportional to the current density at the position of the vortex.

As a result of these calculations the expression for the I–V characteristics of wide but short bridge contacts, as has been shown in Ref. 24, can be written as

$$I - I_c = I_c\left(\frac{2\xi}{w}\right)^{1/2}\sum_m q_m\left[\frac{(w/2) + x(m\pi\hbar/e\langle V\rangle)}{(w/2) - x(m\pi\hbar/e\langle V\rangle)}\right]^{1/2}, \tag{1.12}$$

where $\langle V\rangle$ is the average voltage on the contact and $x_m = x(m\pi\hbar/e\langle V\rangle)$ is the coordinate of the mth vortex. In this model the critical current is determined by the force of the interaction of the vortex with the edge of the bridge. If the current through the contact is changed, then the number of vortices in it are also changed, which results in a change in the number of terms in formula (1.12). Kinks then appear on the I–V characteristics (Fig. 4). A qualitative picture of the generation of a vortex can be seen in the following way. At any instant of time a superconducting current equal to its maximum critical value flows through the contact, along with a normal current ΔI. The electric field that is produced at the edge of the contact causes a phase change $\Delta\varphi$ in the order parameter and a decrease in the superconducting current by an amount proportional to $(\Delta\varphi)^2$. The time t over which the superconducting current decreases and the normal current correspondingly increases by an amount $\sim\Delta I$ can be found from the condition $\Delta\varphi/t\sim\Delta I\sim(\Delta\varphi)^2$. Therefore, $t\sim(\Delta I)^{-1/2}$. A further phase change, resulting in the formation of a vortex, occurs very rapidly. Hence, the characteristic time for the formation of a vortex in the contact is

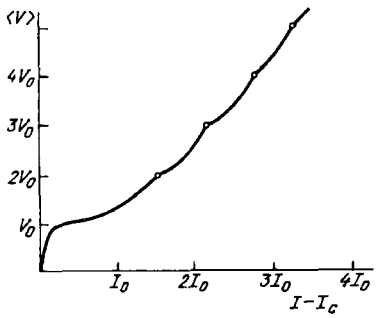

FIG. 4. Current-voltage characteristic of a vortex contact (Ref. 24).

$t_0 \sim (\Delta I)^{-1/2}$. This time does not depend on the size of the contact. Since, if $\Delta I/I_c \ll 1$ it is determined only by the width of the contact and does not depend on the bias current, in this limit the period of vortex motion is equal to the time of formation of a vortex. Because the average voltage is inversely proportional to this period, $\langle V \rangle \sim (\Delta I)^{1/2}$, the shape of the I–V characteristic is the same as for small ridges, that is, it is hyperbolic.

For large currents ($I \gg I_c$) another approximation is valid for the I–V characteristics:

$$\langle V \rangle \sim A(T) I^2, \tag{1.13}$$

where

$$A(T) = 128\hbar \lambda^2(T)/c^2 e w^2 d\eta(T). \tag{1.14}$$

This shape of the voltage vs current curve can be accounted for by the following reasoning. Relation (1.2b) is a very general one in superconductivity, and the passage of each vortex makes a change of 2π in the order parameter at two points of the "banks" sufficiently far from the bridge. In this way, one finds that the average voltage is proportional to the total number of vortices in the contact and inversely proportional to the time for a vortex to move through it, while both of these quantities are proportional to the current passing through the contact. Here it is assumed that the vortices do not move very fast, so that the coefficient of viscosity η does not depend on the current.

If a constant current passes through the contact, a periodic alternating voltage can be generated in it, with a period t_g that depends on the time of motion of the vortex chain. This voltage can be expanded in a Fourier series:

$$V(t) = \sum_{k=-\infty}^{\infty} V_k \exp\left(-\frac{2\pi i k t}{t_g}\right), \tag{1.15}$$

$$V_k = \frac{2\hbar}{et} \int_0^{t_g} \sum_m \frac{q_m x_m(t)}{(w^2 - 4x_m^2(t))^{1/2}} \exp\left(\frac{2\pi i k t}{t_g}\right) dt, \tag{1.16}$$

where $x_m(t)$ is the coordinate of the mth vortex at time t. For currents that are close to I_c the voltage spectrum is full of harmonics. As the current increases the amplitude of the first harmonic increases and the amplitudes of the higher harmonics decrease.

If the contact is placed in an external alternating electromagnetic field with a frequency ω the total current through the contact acquires an alternating component

$$I(t) = I + I_\omega \sin(\omega t + \delta). \tag{1.17}$$

In this case the condition for the generation of each new vortex is given by formula (1.9) as before. However, the quantity $I(t_n) - I_c$ should be substituted on the left-hand side of this formula, where $I(t_n)$ is now the total current at the time of generation of the nth vortex.

When the frequency ω of the external radiation is a multiple of the frequency of the motion of the vortices, then, as before, the vortices are created in equal time intervals $T = (2\pi k/\omega)$. Here the average voltage $\langle V \rangle$ is related to the frequency ω of the external field by $\langle V \rangle = \hbar\omega/4\pi e k$. Equation (1.12) becomes

$$I + I_\omega \sin\delta = I(\hbar\omega/2tk), \tag{1.18}$$

where the right hand side is the current corresponding to the voltage $\hbar\omega/2ek$ in the absence of an alternating current. It is clear that, depending on the phase δ of the current at the instant of creation of a vortex, the average current through the contact can take on different values for the same voltage. This means that there is a step of width $2I_\omega$ on the I–V characteristic at the voltage $\hbar\omega/2ek$.

An analogy to wide bridge contacts with Josephson structures also is found in the investigation of the effect on these devices of an external magnetic field. The dependence of the critical current of microbridges on the external magnetic field has been calculated in Ref. 23. Since the "Meissner" state is destroyed when $H \neq 0$ because of the creation of vortices oriented along the field, the curve of $I_c(H)$ also oscillates in a manner like that of the analogous curve for a tunneling Josephson junction. The period of the oscillations is determined by the magnetic flux quantum ($\phi_0 = \pi c\hbar/e$) divided by the area of the bridge. In the present investigation the pinning of Abrikosov vortices was not taken into account, and the critical current was determined from the condition of the interaction of the vortices with the boundaries of the microbridge.

The asymmetry of the contact results in the following change in the pattern of motion of the vortices: the vortices will be created only at one edge of the contact, pass entirely through the region of the contact, and disappear at the other edge. As a consequence, the asymmetry changes the numerical coefficients in the functions presented above.

Most of the results of these theoretical investigations have been verified experimentally. The work of Ref. 26 may be cited in this connection; there a Pb–Nb–Pb bridge of variable thickness was studied. The experimenters used ion implantation to weaken the order parameter in the niobium microbridge. Table I lists the parameters of the bridges that they studied (d_b means the thickness of the bands of the microbridge).

The I–V characteristics and the curves of $I_c(T)$ were found to be in good agreement with the curves calculated theoretically from relation (1.12). The high-frequency properties of these bridges are evidence for the coherent single-line motion of the vortices in the bridges. Crozat *et al.*[26] measured the emission at 2 GHz generated by these bridges. A somewhat unexpected result was the behavior of the amplitudes of the steps formed on the I–V characteristics by irradiation with electromagnetic radiation; it proved to be close to that obtained theoretically for the resistive model. This common behavior of vortex bridges and microbridges

TABLE I.

Bridge	d, nm	d_b, nm	l_m, μm	w, μm	T_c, K	R, Ω	$\xi(0)$, nm	$\lambda_\perp(0)$, nm
124B2	33	800	1,2	1,2	6,8	7	8,5	750
110C2	33	600	4,5	1,8	6,6	15	8,5	750
143A1	33	800	0,8	2	6,2	4,5	7,5	1200

small compared to the coherence length requires further clarification.

Complex phenomena, in particular the formation of current steps on the I–V characteristics at voltages given by relation (1.3), have been observed in microbridges of large dimensions made of type I superconductors. The resistive state in these materials is due to the motion of flux tubes. These tubes are formed by the coupling of quantized magnetic vortices that are generated in the bridges by the bias current. The dimensions of these tubes reach tens of microns, so that it is possible to see their motion by magnetooptical methods.[27]

1.3. Microbridges made of superconductors with high critical temperatures

Microbridges made of high-temperature (high-T_c) superconductors and having dimensions that are large in comparison with coherence lengths are of considerable interest because they exhibit the properties of Josephson junctions at high temperatures.[28–42] When they are placed in a microwave field their I–V characteristics have current steps at voltages given by the usual Josephson relation (1.3), and it has been found that they can be used to make SQUIDs. This list of publications is far from complete. A more complete list of publications dealing with the Josephson effect at contacts of high-T_c superconductors can be found in the review of Likharev and Kupriyanov.[43]

It has been established that the high-T_c superconductors are of type II, with an extremely short coherence length,[2] about 10 Å. Prior to the discovery of the high-T_c superconductors, microbridges of NbN (Refs. 27–30) and superconductors of the A15 structure[23,31–36] were studied in great detail. These superconductors, as is the case for the recently discovered high-T_c superconductors, have a short coherence length: $\xi_0 \sim 30$–40 Å (Ref. 44) and relatively high critical temperatures, up to 23.2 K for Nb_3Ge. Such short coherence lengths make it extremely difficult to make bridges with constrictions that are smaller than $\xi(T)$. One can use two approaches to analyze the properties of contacts made of superconductors with high critical temperatures. One of them, described above, is the usual vortex mechanism, with allowance for the high operating temperatures and the short coherence lengths. The second approach is based on the fact that these superconductors, especially in the case of bulk high-T_c samples, are easy to prepare in granular form. They consist of a conglomerate of anisotropic granules separated by nonstoichiometric interlayers, a form that is due to the details of the synthesis (they are prepared by a solid-state chemical reaction at high temperatures), and to the complexity of the crystal structure. These samples can be regarded as a collection of superconducting granules electrically coupled by Josephson junctions. The complex granular structure is found ordinarily in high-T_c superconductor films. The granularity of the superconducting samples has a strong influence on their electromagnetic properties. Moreover, to weaken the link between the banks and to localize the processes better, microbridges made of these materials usually receive additional treatment. The techniques used for this purpose are erosional treatment by passing microsecond current pulses through the bridges,[32] radiation treatment,[31] and controlled ion etching.[30] As a result, additional inhomogeneities with dimensions comparable to the coherence length are formed in the microbridge, which might be responsible for the typical Josephson behavior of these contacts. Nevertheless, this does not diminish the importance of studying ordinary microbridges with constriction dimensions considerably larger than the coherence length, particularly since these contacts exhibit some similarity to the usual Josephson junctions.

Besides their similarity to ordinary Josephson junctions, microbridges based on epitaxially grown high-T_c films and superconductors with the A15 or B1 lattice are different from them in some important ways. For example, they have an unusual temperature dependence of the critical current. We recall that $I_c(T)$ of tunneling Josephson junctions and microbridges with small constriction dimensions varies linearly, $I_c(T) \sim T_c - T$, near T_c. In microbridges with a short coherence length a power-law relation has been observed, $I_c(T) \sim (T_c - T)^\alpha$, where the exponent α can have various values, 1.25, 1.5, 2, or 2.5. Various I–V characteristics have been observed in the autonomous regime by various investigators. For example, in microbridges made of NbN and Nb_3Sn I–V characteristics have been observed[28,30] very close to a hyperbolic shape, $\langle V \rangle \sim (I^2 - I_c^2)^{1/2}$. In a number of papers[33–36] these characteristics, on the other hand, had a parabolic shape, close to the form $\langle V \rangle \sim I^2$.

In experiments with microbridges made of NbN, A15, and B1 superconductors, another limiting case is usually obtained, where w and l_m are both $\gg \xi(T)$. In this limit the critical current is determined not by the interaction of the vortices with the contact boundaries, but by the interaction with inhomogeneities in the superconductor. Thus, in addition to the radiophysics aspects, there is a considerable amount of pinning of Abrikosov vortices in these microbridges. The necessity of taking this phenomenon into account was first pointed out by Janocko *et al.*[29] in their investigation of NbN microbridges. The most obvious demonstration of the effect of pinning on the behavior of these microbridges is the dependence of the critical current on the magnetic field (Fig. 5), which is typical of type II superconductors and completely different from the analogous dependence for Josephson junctions.[23]

By taking into account the pinning of Abrikosov vortices one can explain the similar behavior of the microbridges.[45] The Josephson properties of the contacts in these experiments was accounted for by analogy with Ref. 24, with a single essential difference—the interaction of the vortices with the inhomogeneities within the bridge was taken into

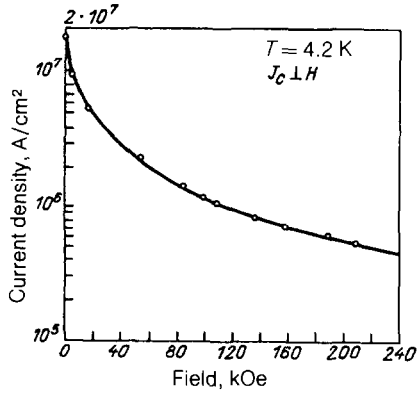

FIG. 5. Magnetic field dependence of the critical current of a NbN bridge for $T = 4.2$ K (Ref. 29).

account, not the interaction with the edges of the bridge. The microstructure of bridges made of films of intermetallic compounds consists of a collection of small ($< 10^3$ Å) columnar grains, whose boundaries are vortex pinning centers. For ordinary currents passing through the microbridge ($\leqslant 1$ mA) an estimate of the self-magnetic field shows that in the absence of an external magnetic field there is only a small number of vortices spaced apart in a chain at a distance much greater than the size of the grains. If we neglect the elastic interaction between the vortices and the lattice, then the bulk pinning force can be found by a direct summation of the elementary pinning forces, which depend on the nature and size of the inhomogeneities. To estimate the elementary pinning force it is assumed that the size of the inhomogeneity in the plane of the film is smaller than the coherence length but larger than the radius of action of the kernel that figures in the equation of self-consistency for the determination the energy gap in the excitation spectrum. In this case we obtain

$$f_p(T) \sim H_c^2(T)\delta V/8\pi\xi(T); \tag{1.19}$$

where δV is the volume of the inhomogeneity, which is some kind of non-superconducting inclusion. This formula is obtained by dividing the energy gain of the superconductor when a vortex passes through the inhomogeneity by the characteristic distance over which this energy varies. The energy difference will be greater if the inhomogeneity has dielectric properties. The critical current of the bridge in this case is determined by the equality of the Lorentz force, which tends to break the vortex loose from the inhomogeneity, and the pinning force, which holds it there. The condition for the separation of a vortex gives a critical current $I_c(T) \sim cwf_p(T)/\phi_0 \sim (T_c - T)^{2.5}$. In the limit $\lambda(T)/\xi(T) \gg 1$, which is satisfied by all superconductors with high critical temperatures, this "core" pinning mechanism is very effective. If it is assumed that the inhomogeneities are thin planes perpendicular to the plane of the film and oriented along the direction of current flow through the bridge, then $f_p(T) \sim H_c^2(T) \sim (T_c - T)^2$. If it is assumed that the dimension of the inhomogeneities exceeds the coherence length, then $f_p(T) \sim H_c^2(T)\xi(T) \sim (T_c - T)^{1.5}$. As the temperature approaches the critical temperature, where the effectiveness of the pinning centers falls off sharply, the critical current must be determined from the condition of entry of a vortex into the bridge, that is, its interaction with the boundaries of the bridge. In this case the nature of the function $I_c(T)$ must change: from $I_c(T) \sim (T_c - T)^{2.5}$ at low temperatures to $I_c(T) \sim (T_c - T)^{1.25}$. In this way, the experimentally determined temperature dependence of the critical current of bridges made of high-T_c superconductors can be easily explained.

To find the shape of the I–V characteristics in this case one must take into consideration not only the viscous motion of the vortices, but also the thermally activated flux creep. Experiments carried out with bulk samples of Pb–In and Nb–Zr have shown that for $T \approx 0.5T_c$ the value of $U/k_B T$ is 10^2–10^3, where k_B is the Boltzmann constant and U is the depth of the potential well of the pinning center.[46] Therefore, the probability of thermal hopping of a vortex from one pinning center to another is extremely low. It is another situation for superconductors with a high critical temperatures and short coherence lengths for a number of reasons:

a) In bulk superconductors bound vortices, consisting not of a single vortex, but sometimes 10^2–10^3 vortices, are coupled together, so the vortex pinning energy must increase in about the same proportion.

b) Measurements of the I–V characteristics in microbridges have usually been carried out near T_c, which for the high-T_c superconductors is very high, and thus increases the energy $k_B T$ of the thermal fluctuations.

c) The coherence length is short, and consequently, because of the relation $I_c \sim U/\xi$, the critical current can be large when the wells are shallow.

It is of particular importance to take into account the thermal activation of flux creep in high-T_c superconductors, where it even affects the temperature dependence of the upper critical magnetic field.[47] In the work of Anderson,[48] analyzing the behavior of bulk type II superconductors in a uniform magnetic field, it was shown that for currents smaller than the critical current as determined from the condition of equality of the pinning force and the Lorentz force, hopping motion of vortices from one potential well to another, that is, from inhomogeneity to inhomogeneity, is possible on account of thermal fluctuations. An electric field is produced because of this vortex motion. Anderson derived the following formula for the electric field strength:

$$E = v_0 B \exp[-U(T)(1 - I \cdot I_{c0}^{-1})/k_B T]/c, \tag{1.20}$$

where I_{c0} is the critical current in the absence of fluctuations and v_0 is a quantity having the dimensions of velocity. This quantity is not well known. On the basis of formula (1.20) it is possible to calculate the form of the I–V characteristics of wide bridge contacts made of type II superconductors in the case we are considering, where the critical current is determined by the pinning of individual vortices. A particularly simple formula can be derived in the limit where the distance between the pinning centers is much greater than the coherence length. In this case, the time that a vortex remains in a contact, which is determined by the voltage across the contact, is made up of the time it remains at the pinning center plus the time of viscous motion through the contact if there were no inhomogeneities in the contact. The residence time in pinning centers can be estimated from formula (1.20). Since there are usually a large number of such centers in a bridge of micron size, the total time residence τ at the cen-

ters is the sum of the times that the vortex is located in all the pinning centers, where the residence time of a vortex in the ith potential well is

$$\tau_i \sim \exp[U_i(1 - I \cdot I_{ci}^{-1})/k_B T]. \quad (1.21)$$

If a bridge contains strong pinning centers, for which $U_i/k_B T \gg 1$, then the main contribution to the total time will come only from those centers

$$\tau \sim \exp[U_{max}(1 - I \cdot I_{c,max}^{-1})/k_B T]. \quad (1.22)$$

This follows from the fact that in the limit $U_{max}/k_B T \gg 1$ the effect of creep on the form of the I–V characteristics will be significant only if $1 - I \cdot I_{c,max}^{-1} \to 0$, that is, if $I \to I_{c,max}$. For this current through the junction the quantity $1 - I \cdot I_{ci}^{-1}$ will be considerably different from zero for the shallower pinning centers, so that $\tau_i \ll \tau_{max}$. Henceforth the subscript max will be omitted.

The time of viscous motion of the vortices through the contact in the absence of inhomogeneities can be found from Ref. 24. If it is assumed that the pinning force is usually greater than the force of interaction with the boundaries of the bridge, it can be shown that the I–V characteristics will have the following shape:

$$V = A(T)I^2\{1 + A(T)I \exp[U(T)(1 - I \cdot I_{c0}^{-1})/k_B T]/R_0\}^{-1}, \quad (1.23)$$

where $R_0 = v_0 l_m/wc^2$ and $A(T)$ is given by formula (1.14). From expression (1.23) it follows that if thermal fluctuations are taken into account the voltage across the contact is also different from zero for currents less than I_{c0}. In order for this effect to be appreciable, the ratio between the depth of the potential well and the energy of the thermal fluctuations $k_B T$ must not be too large. Estimates show that this case occurs not only in thin-film bridges made of the high-T_c superconductors, but also in superconducting bridges made of the A15 or B1 material. For currents that exceed I_{c0} formula (1.23) rapidly tends to a quadratic dependence $V \approx A(T)I^2$. For currents small compared to I_{c0} the equation for the I–V characteristics is close to formula (1.20). Experimental confirmation has been obtained in Refs. 42 and 49 for the existence of thermally activated flux creep in microbridges made of A15 superconductors and in microbridges prepared from epitaxial films of $YBa_2Cu_3O_{7-x}$. Good agreement was obtained between the I–V characteristics and formula (1.23). Figure 6 shows an example of a curve of V/I as a function of the bias current for a $YBa_2Cu_3O_{7-x}$ microbridge.[42] The quantity V/I is plotted on a logarithmic scale. In agreement with formula (1.23), the function $\ln(V/I)$ plotted against I is linear for small voltages. Moreover, using these curves, Zhukov *et al.*[42] were able to determine the depth of the potential wells. Previously, a similar dependence was obtained for microbridges made of superconductors with the A15 lattice.[45]

By the use of pinning, one can explain effects typical of Josephson junctions in microbridges of type II superconductors. For example, the superconducting quantum interference can be explained by the periodic penetration of quantized magnetic vortices into the superconducting loop. It is more interesting to analyze the role of pinning in effects that are similar to the ac Josephson effect.[45] In this case the current steps at voltages of $n\hbar\omega/2e$ are formed because the times of separation of the vortices from the pinning centers are synchronized by the microwave radiation. The total current passing through the junction in a microwave field can be written in the form (1.17). The equation that determines the time of separation of the vortices from this center is

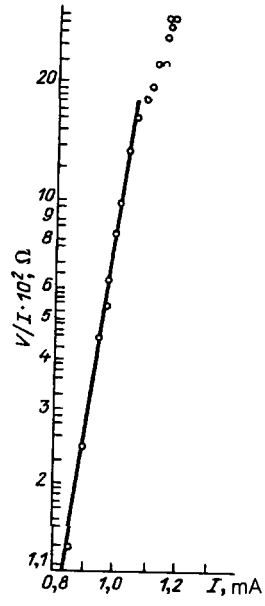

FIG. 6. The function $\ln(V/I)$ plotted against I in the autonomous regime (Ref. 42).

$$F_n(t) + F_d(t) = f_p, \quad (1.24)$$

where F_n is the Lorentz force, which is proportional to the current through the contact and F_d is the force acting on a vortex by those previously separated. When the voltage on the contact is close to $n\hbar\omega/2e$, then because of the additional synchronization induced by the microwave radiation in the times of separation of the vortices from the pinning centers, the separation frequency, and consequently the voltage on the contact does not change with a change in the transport current. For this reason a current step appears on the I–V characteristic.

The number of Abrikosov vortices in a bridge can be varied by an external magnetic field. The synchronization condition for the motion of the vortices in contacts of large dimensions can be considerably altered. In Ref. 50 it was observed that a weak magnetic field (~ 10 G), which has little effect on the critical current, completely suppresses the Josephson step structure in the I–V characteristics of large microbridges prepared of Nb_3Sn. This effect is a result of the fact that in bridges with large dimensions the synchronization of the vortex motion is hindered when there are a large number of them in the bridge.

As was remarked previously, the second method of analyzing the properties of microbridges made of superconductors with a high critical temperature is based on the fact that they are easily prepared in granular form. A large number of theoretical and experimental investigations have been carried out on granulated superconductors based on Al, NbN, and Sn.[51–53] If the Josephson coupling between the granules

is strong, that is, if the current passing between them is able to suppress the order parameter in the granules, then these superconductors can be regarded as ordinary "dirty" superconductors. In this case, their resistive properties are determined by the interaction of the Abrikosov vortices with the inhomogeneities in the samples. In the case of a weak link between the granules, the Josephson current between the granules is small and it can have no effect on the order parameter in the granules. By creating a constriction in a superconducting film, one can see that the contact between the banks is made through a small number of granules. In the case of high-T_c superconductors the situation arises where the contact is made by no more than two granules.[54,55] This possibility is interesting for applied purposes. As a result, the usual Josephson relation (1.28) is valid for the critical current, that is, the contact will have classical Josephson properties. One of the distinguishing features of these contacts is the rapid falloff of the critical current in a magnetic field.[56] The Josephson behavior of bridge contacts in the case of granular samples has been observed many times, both for the high-T_c superconductors and for microbridges based on superconductors with the A15 lattice or NbN (Refs. 25, 27). In addition, there have been experiments carried out on single-crystal films, in which ordinary vortex behavior has been observed.[39,57]

Even though the vortex bridge contacts are inferior to Josephson junctions in terms of their radiophysical properties, nonetheless their study is of great interest. From the theoretical point of view they are interesting because their dimensions are small so that the analysis of the vortex behavior in them is simpler than it is in ordinary bulk superconductors, and as a result, their study can yield information on the elementary interactions of the Abrikosov vortices with inhomogeneities in the superconductor. The vortex bridges are also interesting from the experimental point of view, since they exhibit beautiful coherence effects that resemble the Josephson effect. Further progress in this direction depends on the technology of preparing the microbridges. In particular, by making contacts with sharply defined geometric dimensions it will be possible to determine more accurately the depth of the potential wells of the pinning centers and the motion of the vortices.

2. THIN-FILM MULTIELEMENT MICROSTRUCTURES

2.1. Vortices in thin-film superconductor films

2.1.1. Weak magnetic fields

First of all, let us recall the properties of Abrikosov vortex structures in thin films ($d \ll \lambda$; Ref. 58). Within the superconducting film the following equation in cylindrical coordinates is valid for the vector potential

$$\nabla^2 \mathbf{A} = \lambda_\perp^{-1}(\mathbf{A} - \mathbf{\Phi})\delta z, \tag{2.1a}$$

$$\mathbf{J} = -\frac{c}{4\pi\lambda_\perp}(\mathbf{A} - \mathbf{\Phi}), \tag{2.1b}$$

where the Z axis is perpendicular to the surface of the film and $\mathbf{\Phi}$ is a vector with the components $\Phi_r = \Phi_z = 0$ and $\Phi_\theta = \phi_0/2\pi r$. Since in this case the current can be screened only within the thickness of the film, the magnetic field can penetrate a much larger distance than in the bulk superconductor. Solving equations (2.1a) and (2.1b), we can find the current distribution around the vortices:

$$\langle \mathbf{J}(r) \rangle = c\phi_0 [H_0(r/2\lambda_\perp) - Y_0(r/2\lambda_\perp) - (2/\pi)]/32\pi\lambda_\perp, \tag{2.2}$$

where H_0 and Y_0 are the Struve and Neumann functions, respectively. The magnetic part of the vortex energy ε_M per unit length of the vortex is given by the integral

$$\varepsilon_M = \frac{1}{8\pi}\iint_{r>\xi}\left[\mathbf{h}_M^2 + \frac{1}{d}\left(\frac{4\pi}{c}\right)^2 \lambda_\perp \mathbf{J}^2\right] dx dy$$
$$\approx \frac{1}{\lambda_\perp d}\left(\frac{\phi_0}{4\pi}\right)^2 \left(\ln\frac{4\lambda_\perp}{\xi} - \gamma - \frac{1}{2}\right), \tag{2.3}$$

where γ is the Euler constant and $\mathbf{h}_M = \text{curl } \mathbf{A}$ is the local magnetic field near any vortex. The latter expression was derived in the limit $\lambda_\perp \gg \xi$. Here the energy of condensation (ε_c) per unit length of a vortex is given approximately by the relation

$$\varepsilon_c = \iint_{r \le \xi} \frac{H_c^2}{8\pi} dx dy = \frac{1}{4\lambda_\perp d}\left(\frac{\phi_0}{4\pi}\right)^2, \tag{2.4}$$

while the self-energy U_n of a vortex is determined by the sum of these energies:

$$U_n = (\varepsilon_M + \varepsilon_c)d = \varepsilon d, \tag{2.5}$$

where ε is the self-energy per unit length of a vortex.

Unlike the case for bulk superconductors, the interaction between vortices in thin films is long-range, and the following expression holds for the interaction potential between two vortices aligned in the same direction:

$$W(r) = \phi_0^2 [H_0(r/2\lambda_\perp) - Y_0(r/2\lambda_\perp)]/16\pi\lambda_\perp = dW_i, \tag{2.6}$$

where W_i is the interaction energy per unit vortex length. Two approximations come from relation (2.6). For $\xi(T) \ll r \ll \lambda_\perp(T)$,

$$W(r) = -\phi_0^2 \ln(r/\xi)/8\pi^2\lambda_\perp, \tag{2.7}$$

and for large distances ($r \gg \lambda_\perp$)

$$W(r) = \phi_0^2/4\pi^2 r, \tag{2.8}$$

i.e., the interaction between the vortices does not fall off exponentially as it does in bulk superconductors, but considerably slower. The cause of this difference is that in thin films the vortices interact not only in the film itself, but through the space surrounding the film.

Another important difference between the vortex structures in the interior of a superconductor and those in a film is that in the latter case below the upper critical magnetic field H_{c2} the magnetic induction B is close in value to the external magnetic field down to very small magnetic fields. Moreover, because the thickness of a superconducting film is finite, the vortex structure is three-dimensional, unlike the two-dimensional structure in a bulk superconductor. The situation is considerably simplified for a thin film ($d \ll \xi, \lambda$) where one can neglect the variation of the order parameter $\psi(r)$ and the local magnetic field $\mathbf{H}_l(\mathbf{r})$ transverse to the film.

2.1.2. Strong magnetic fields

Tinkham[59] first noted the possibility of a vortex structure in thin films. At low temperatures the vortices form a three-dimensional lattice with a period given by the relation

$$(\sqrt{3}/2)a_0^2 = \phi_0/B.$$

An accurate investigation of the mixed state in thin films has been made by Maki.[60] In the study of the mixed state in superconductors it is frequently convenient to use reduced units: lengths in units of λ, energy density in units of $H_c^2/4\pi$, magnetic fields in units of $\sqrt{2}H_c$, and current density in units of $\sqrt{2}H_c/4\pi\lambda$. The Ginzburg–Landau free energy functional $\mathcal{F}$ for such a film is written as

$$\mathcal{F} = \int d^3r'\{H'^2 + g(z)[-|\psi|^2 + \frac{1}{2}|\psi|^4 + \left|\left(\frac{\partial}{i\varkappa\partial \mathbf{r}} - \mathbf{A}\right)\psi\right|^2]\},$$
$$g(z) = \begin{cases} 1 & \text{for } 0 < z < d, \\ 0 & \text{for } z \le 0 \text{ and for } z \ge d, \end{cases} \tag{2.9}$$

where $\mathbf{r}$ is a two-dimensional vector in the (x,y) plane of the film. By a variation of the functional (2.9) one obtains equations similar to the Ginzburg–Landau equations for bulk superconductors:[60]

$$\left(\frac{\partial}{i\varkappa\partial \mathbf{r}} - \mathbf{A}\right)^2\psi = \psi - |\psi|^2\psi, \tag{2.10a}$$

$$\text{curl curl } \mathbf{A} = \frac{1}{2}g(z)\left[\psi^*\left(\frac{\partial}{i\varkappa\partial \mathbf{r}} - \mathbf{A}\right)\psi - \psi\left(\frac{\partial}{i\varkappa\partial \mathbf{r}} + \mathbf{A}\right)\psi^*\right]. \tag{2.10b}$$

The appearance of the function $g(z)$ in the case of a thin film dictates that the magnetic field outside the film is three-dimensional. Nonetheless, Eqs. (2.10a) and (2.10b) imply that in thin films, just as in bulk superconductors, a three-dimensional lattice of Abrikosov vortices is formed near the upper critical field (when $H_{c2} - H \ll H_{c2}$). The free energy is given by the expression

$$F = (\mathcal{F} - \int H^2 d^3r)(d\int d^2r)^{-1} = -\frac{(\varkappa - H)^2}{\beta_A(2\varkappa^2 - f^*)}, \tag{2.11}$$

where β_A is a parameter that in the Abrikosov theory of the mixed state[61] determines the energy of the vortex lattice near the upper critical magnetic field:

$$\beta_A = \langle\psi^4\rangle/(\langle\psi^2\rangle)^2, \tag{2.12}$$

and f^* is a function with a value smaller than unity that goes monotonically to zero as the film thickness decreases. Furthermore, that function depends only weakly on the form of the lattice in the film. We recall that in the case of a bulk superconductor the function f^* is replaced by unity.

As is well known, a triangular lattice is isotropic in its elastic properties and is described by the bulk and shear moduli. One of the consequences of the long-range nature of the interaction between vortices in a film is the incompressibility of the vortex lattice in thin films (the bulk modulus is infinite). Since bending strains of the vortices in thin films can also be neglected, only the shear strains will have any significant effect on the behavior of the vortex lattice. The shear modulus is defined as

$$\mu = \partial^2 F/\partial\alpha^2, \tag{2.13}$$

where α is the angle of shear of the vortex lattice. The value of this quantity has been calculated in Refs. 62–65 for various values of the Ginzburg–Landau parameter, various film thickness, and various magnetic field strengths. Returning for convenience to real coordinates, one can write the expressions for the shear modulus in thin films in three limiting cases

$$\mu = (\phi_0 H^3/\pi^5)^{1/2}/32, \quad (\phi_0/H)^{1/2} \gg \lambda_\perp(T), \tag{2.14a}$$

$$\mu = \phi_0 H/64\pi^2\lambda_\perp, \quad \xi(T) \ll (\phi_0/H)^{1/2} < \lambda_\perp(T), \tag{2.14b}$$

$$\mu = 0{,}472d(H_{c2} - H)^2/(2\varkappa^2 - f^*), \quad (\phi_0/B)^{1/2} \ge \xi(T). \tag{2.14c}$$

Thermal fluctuations have a large influence on the properties of a vortex lattice, and this influence is particularly strong in the case of thin films. It has been observed that at finite temperatures not only can the vortices oscillate about their equilibrium positions, but the lattice can even melt and transform to the liquid state.[66] The condition for the melting of a vortex lattice is given by the relation

$$\mu(T_M)a_0^2/k_B T_M = 4\pi, \tag{2.15}$$

where T_M is the melting point of the vortex lattice. In zero magnetic field a transition from the superconductor state to the dissipative state is also possible via the motion of vortices formed in the film as a result of thermal fluctuations.

2.2. Experimental results obtained with superconducting films with longitudinal corrugations

When a film is of nonuniform thickness, the vortices, tending to minimize the energy, occupy the regions where the film is the thinnest. If the thickness of the film varies randomly in space, then distortions will be formed in the regular triangular vortex lattice. The situation is different if the variation of the film thickness in space is strictly periodic. The first experiments on the effect of an ordered surface relief on the pinning of vortices were carried out by Morrison and Rose.[67] These investigators used a diffraction grating to impress grooves with a triangular cross section on the surface of an In-2% Bi alloy sample. They measured the critical current passing along the grooves in a magnetic field perpendicular to the sample surface. According to their results, the bulk pinning force is directly proportional to the blaze angle of the grooves and inversely proportional to their spacing. If the grooves are narrower than the coherence length they have little influence on the magnitude of the pinning. The explanation for the pinning mechanism proposed in that paper was based on the increase in the energy of the vortex as it moves along the sloping side of a groove, a result that follows from formula (2.5).

A large series of investigations has been carried out by Martinoli and his coworkers on the mixed state in corrugated superconducting films.[68–73] They used aluminum films deposited in an oxygen atmosphere. These films have a very small amount of random pinning. Because of their high resistivity and small thickness, the effective magnetic field penetration depth is greater than the film thickness. Therefore, the interaction between the vortices is long-range, even though the London penetration depth λ_L in aluminum is small. The corrugations in these experiments were usually

produced in the following way. The deposited aluminum film was coated with a photosensitive material and then grooves were formed in this photosensitive layer by the interference of two He-Cd lasers. After this photosensitive layer was given the appropriate treatment, the aluminum film was etched to produce the desired profile.

In a magnetic field given by the relation

$$B_{nk} = \frac{\sqrt{3}\phi_0}{2\lambda_g^2(n^2 + nk + k^2)}, \tag{2.16}$$

where n and k are integers, the vortex lattice coincides with the corrugation. In the commensurate phase, where all the vortices are located in the depressions, the vortex lattice is undistorted and the bulk pinning force is equal to the sum of the elementary interactions of each vortex with the inhomogeneities of the film. In the experiment this showed up in peaks in the curve $I_c(B)$ at $B = B_{nk}$ (Fig. 7), when the transport current flows along the corrugation lines.[68] In that experiment the corrugated film was of aluminum $\sim 0.5\ \mu$m thick with a corrugation depth of 200 Å and a period $\lambda_g = 1.9\ \mu$m.

If the transport current flowing parallel to the corrugations exceeds the critical current I_c, then viscous flow of the vortex lattice occurs. In the general case of $B \neq B_{nk}$ the interaction between the vortices and the periodic pinning structures distorts the vortex lattice, but if $B = B_{nk}$ these distortions are not present and the vortices move synchronously in identical pinning fields. The viscous motion of vortices in corrugated films was studied experimentally in Ref. 69 with films similar to those of Ref. 68. An effect was observed, related to the ac Josephson effect. Current steps were formed on the I–V characteristics when the films were irradiated in an external electromagnetic field with $B = B_{10}$ (Fig. 8). The positions of these steps were given by

$$E_{mn} = n\omega\lambda_g B/2\pi mc, \tag{2.17}$$

where n and m are integers.

In addition, Martinoli and his coworkers[70] detected electromagnetic radiation directly as the vortex lattice

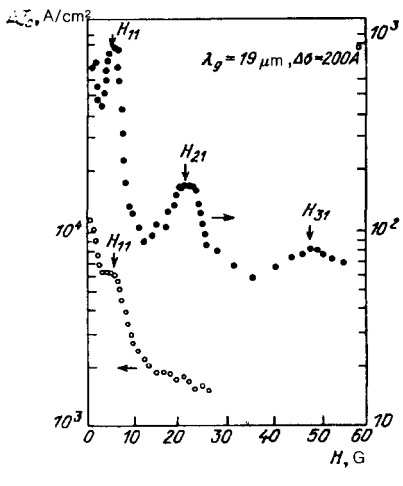

FIG. 7. Critical current density as a function of the magnetic field for a corrugated Al film (Ref. 68).

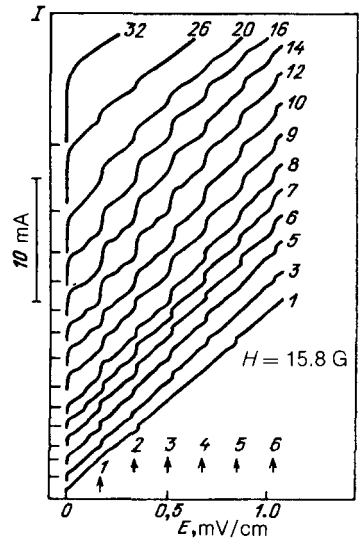

FIG. 8. I–V characteristics of a corrugated Al film in an rf field. The numbers on the curves indicate the attenuation in dB of the power of the electromagnetic radiation. The critical current of the film is 6.4 mA, the amplitude of the rf current without attenuation is 70 mA. The curves are vertically shifted along the current axis (Ref. 69).

moved in the corrugations of the film. It was found extraordinarily difficult to produce coherent motion of the vortices, so that the generated power was small ($\sim 10^{-15}$ W) and frequency range (30–50 MHz) in which the radiation was produced was narrow. These results indicate that ordered motion of the vortex lattice is possible only if the velocity is low. Therefore, it is an important matter to discover the mechanism responsible for the instability of the vortex lattice. One such mechanism is the destruction of the order of the vortex lattice by random pinning centers. A natural means of overcoming this difficulty is to use more perfect films, that is, films with only a small amount of random pinning forces.

2.3. Theoretical models of the interaction of a vortex lattice with corrugated films

2.3.1. Statistical interaction of a vortex lattice with a corrugated film in weak magnetic fields

1) $\lambda_\perp \ll \lambda_g$. A phenomenological model based on the work of Pearl[58] has been developed by Martinoli *et al.*,[71] and describes the static and dynamic properties of vortex lattice in corrugated films. It was assumed that the film is very thin $[d \ll \lambda(T)]$, and its thickness varies sinusoidally:

$$d(\mathbf{r}) = d + \Delta d \cos[\mathbf{q}(\mathbf{r} - \mathbf{r}_0)], \tag{2.18}$$

where $\mathbf{q}$ is the wave vector of the modulation ($|\mathbf{q}| = 2\pi/\lambda_g$) and Δd is its amplitude, with $\Delta d/d \ll 1$, while the vector $\mathbf{r}_0$ gives the position of the vortex lattice relative to the corrugation. For simplicity we assume that $\lambda_g \ll \lambda_\perp$ and $\varkappa \gg 1$. In this case the self-energy of a vortex is given by relation (2.5), while the formula for the interaction energy $W_{ll'}$ of two vortices located at $\mathbf{r}_l$ and $\mathbf{r}_{l'}$ is similar to expression (2.6):

$$W_{ll'} = \frac{\pi\phi_0^2}{2(4\pi\lambda)^2}\{d(\mathbf{r}_l)[H_0(r_{ll'}/2\lambda_\perp(\mathbf{r}_l)) - Y_0(r_{ll'}/2\lambda_\perp(\mathbf{r}_l))] + d(\mathbf{r}_{l'})[H_0(r_{ll'}/2\lambda_\perp(\mathbf{r}_{l'})) - Y_0(r_{ll'}/2\lambda_\perp(\mathbf{r}_{l'}))]\}, \tag{2.19}$$

where $r_{ll'} = |\mathbf{r}_l - \mathbf{r}_{l'}|$. $r_{ll'} \gg \lambda_\perp$ the interaction between the vortices is given by relation (2.8) and does not depend on the thickness of the film. It follows from expression (2.19) that the free energy density of the system is given by

$$f = f_0 + \frac{1}{2A_f} \sum_{\mathbf{q}} \{\Delta\varepsilon \sum_l \exp[i\mathbf{q}(\mathbf{r}_l - \mathbf{r}_0)] + \frac{1}{4} \sum_{\substack{l,l' \\ (l \neq l')}} \Delta W_{ll'} [1 + \exp(-i\mathbf{q}\mathbf{r}_{ll'}) \exp[i\mathbf{q}(\mathbf{r}_l - \mathbf{r}_0)]\}, \tag{2.20}$$

where f_0 is the free energy density for a smooth film and A_f is the area of the sample. For simplicity two quantities are introduced in formula (2.20):

$$\Delta\varepsilon = (\varepsilon - \lambda_\perp \frac{\partial\varepsilon}{\partial\lambda_\perp}) \frac{\Delta d}{d}, \tag{2.21}$$

$$\Delta W_{ll'} = \left(W_{ll'} - \lambda_\perp \frac{\partial W_{ll'}}{\partial\lambda_\perp}\right) \frac{\Delta d}{d}. \tag{2.22}$$

The equilibrium position of the vortices is found by minimizing the free energy with respect to the position. In this way, it is necessary to write for each vortex the following expression

$$\Delta_l f_l = 0. \tag{2.23}$$

Expression (2.20) implies that when the reciprocal lattice vector $\mathbf{g}$ of the vortex structure is equal to the wave vector of the modulation, that is, when

$$\mathbf{q}\mathbf{r}_l = 2\pi n, \tag{2.24}$$

the vortex lattice coincides with the corrugation. Simple calculations show that this equality is satisfied when the magnetic induction is given by formula (2.16). It can be seen from (2.20) and (2.24) that when the vortex lattice matches the corrugation the energy of interaction between the vortices becomes isotropic, since $\exp(i\mathbf{g}\mathbf{r}_l) = \exp(i\mathbf{g}\mathbf{r}_{ll'}) = 1$. Here the free energy density can be written as

$$f = f_0 + \frac{1}{\phi_0} B_{nk} \Delta\varepsilon \cos(qr_0). \tag{2.25}$$

It follows from this expression that the free energy of the vortex lattice, following the corrugation, varies sinusoidally. Since the free energy is a minimum when this coincidence occurs, the function $j_c(B)$ should have maxima. With the use of expression (2.25) one can readily determine the critical current density for this case

$$j_{c,m} = \frac{c}{B_{nk}} \frac{\partial f}{\partial r_0} = \frac{cq|\Delta\varepsilon|}{\phi_0}. \tag{2.26}$$

This formula predicts that the critical current decreases monotonically with increasing temperature in the matching field, at which the coincidence occurs.

The model advanced above, despite its apparent obviousness, has some defects, and consequently there are experimental results that contradict it. For example, Tang *et al.*[73] have observed an anomalous temperature dependence of the critical current of corrugated films (Fig. 9). In these experiments the usual configuration was used, in which the transport current was along the corrugations and the magnetic field $B = B_{10}$ was perpendicular to the surface of the film. The peak on the curve of $I_c(T)$ cannot be accounted for

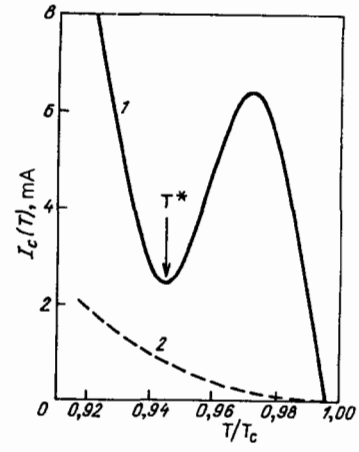

FIG. 9. Anomalous temperature dependence of the critical current of a corrugated superconducting film for $B = B_{10}$ (curve *1*), and for an uncorrugated film (curve *2*) (Ref. 73).

on the basis of expression (2.26). To explain the results the authors studied the action of thermal fluctuations on the vortex lattice. They believed that below the temperature T^* the main influence of the thermal fluctuations is to decrease the order parameter, while above T^* the vortex lattice is softened. As a consequence, the pinning of the vortices at $T \gtrsim T^*$ becomes more effective, and this should produce a peak in the curve of $I_c(T)$.

2) $\lambda_\perp \sim \lambda_g$. Other explanations of this phenomenon are possible. This form of the curve of $I_c(T)$ was predicted by Radovic *et al.*,[74] who studied corrugated films with a period comparable to $\lambda(T)$. In this case Pearl's equations (2.1a) and (2.1b) for the vector potential $\mathbf{A}$ become

$$\nabla^2 \mathbf{A} = \lambda_\perp^{-1}(x)(\mathbf{A} - \mathbf{\Phi})\delta z, \tag{2.27a}$$

$$\mathbf{J} = -\frac{c}{4\pi\lambda_\perp(x)}(\mathbf{A} - \mathbf{\Phi}). \tag{2.27b}$$

The solution of these equations yields

$$\mathbf{J}(\mathbf{r}) = \langle \mathbf{J}(r)\rangle \{1 + \frac{\Delta d}{d} \cos[q(x - x_0)]\} - \frac{cd}{4\pi\langle\lambda\rangle^2} \Delta\mathbf{A}(\mathbf{r}), \tag{2.28}$$

where in this formula and hereafter the average values obtained from Pearl's equations[58] will be used for uniform films. The perturbation of the vector potential, $\Delta\mathbf{A}(\mathbf{r})$, due to the modulation, has been calculated for the general case in Ref. 74. In the limit $r \ll \lambda_g$ it is given by the simple expression

$$\Delta\mathbf{A}(\mathbf{r}) \approx \langle \mathbf{A}(\mathbf{r})\rangle \frac{\Delta d}{d} \cos[q(x - x_0)]. \tag{2.29}$$

In this limit the correction to the magnetic energy is found by analogy with Eq. (2.3) by the integral

$$\Delta\varepsilon_m d = \frac{1}{8\pi} \iint_{r>\xi} \{d\left[\frac{\Delta d}{d}\langle h_M\rangle^2 \cos[q(x - x_0)] + 2(\langle h_M\rangle \Delta h_M)\right] + \left(\frac{4\pi}{c}\right)^2 \frac{\langle\lambda\rangle^2}{d} \left[\frac{\Delta d}{d}\langle \mathbf{J}\rangle^2 \cos[q(x - x_0)] - \frac{cd}{2\pi\langle\lambda\rangle^2}(\langle \mathbf{J}\rangle \Delta\mathbf{A})\right]\} dx dy$$

$$\approx \frac{\Delta d}{d}\langle\varepsilon\rangle J_0(q\langle\xi\rangle) \cos(qx_0), \tag{2.30}$$

$$\Delta\varepsilon_c d = 2\frac{\Delta d}{q\langle\xi\rangle}\langle\varepsilon_c\rangle J_1(q\langle\xi\rangle)\cos(qx_0), \tag{2.31}$$

where $\langle h_M\rangle$ is the local magnetic field near a vortex without the modulation, $\Delta h_M = \mathrm{curl}(\Delta\mathbf{A})$, and J_0 and J_1 are the Bessel functions of the indicated order. Since $\Delta\varepsilon_c \ll \Delta\varepsilon_M$ for a film with a large Ginzburg–Landau parameter $\varkappa$, the correction $\Delta\varepsilon_c$ to the vortex energy can be neglected. As the temperature is changed the Bessel function J_0 also changes. At some temperature T^* defined by the relation $\langle\xi(T^*)\rangle \approx 0.4\lambda_g$, it changes sign. For $T < T^*$ the Bessel function of zero order is positive, $J_0(q\langle\xi\rangle) > 0$, and the energy minimum of the vortices occurs when the condition $\cos(qx_0) = -1$ is satisfied. In this case the vortices tend to occupy the thinnest regions of the film. When $J_0(q\langle\xi\rangle) < 0$, the vortex centers, conversely, tend to occupy the thickest regions of the film. At low temperatures the size of the normal nonsuperconducting vortex core is small in comparison to the period of the corrugation. This situation is close to the limit $\lambda_g \gg \lambda_\perp$ examined in Ref. 71. The energy minimum in this case occurs when the vortices occupy the thinnest regions. When the coherence length becomes comparable to the corrugation period the magnetic energy is governed by the superconducting currents flowing in the regions with the maximum and minimum thickness. Then it is energetically favorable for the vortex centers to be located in the thickest regions.

This unusual temperature dependence of the vortex energy causes the nonmonotonic temperature dependence of the critical current. Its value, as usual, is found from the equality of the Lorentz force with the pinning force resulting in this case from the presence of the corrugations. For $B = B_{nm}$ the following expression is obtained

$$j_{c,m} \approx \frac{c\phi_0\Delta d}{8\pi\lambda_g d\langle\lambda\rangle^2}\left(\ln\frac{4\langle\lambda\rangle^2}{\gamma d\langle\xi\rangle} - \frac{1}{2}\right)|J_0(q\langle\xi\rangle)|. \tag{2.32}$$

Figure 10 shows a plot of $j_{c,m}(T)$ calculated in Ref. 74 using typical values of the corresponding parameters of the superconducting films. This figure shows that there is good agreement between the theoretical curve and the experimental one shown in Fig. 9.

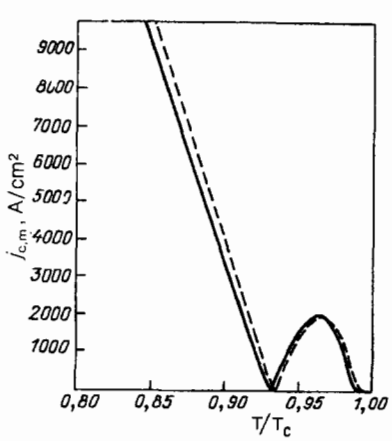

FIG. 10. Critical current density of a superconducting film with parameters $\Delta d/d = 0.1$, $d = 10^3$ Å, $l = 500$ Å, and $\varkappa = 5$, as a function of the reduced temperature. The solid line shows the curve calculated from formula (2.32) and the dashed line the results of calculations with allowance for $\Delta\varepsilon_c$; formula (2.31) (Ref. 74).

The peaks in the curve of $I_c(T)$ can be accounted for by the effect of the magnetic field produced by the transport current, which is usually neglected in comparison to the external magnetic field. The magnetic field of the transport current causes a gradient in the vortex density in the plane of the film, which makes it difficult to match the external magnetic field with the corrugations and decrease the net pinning force. As the temperature is lowered the gradient in the vortex density in the sample increases, which also causes the observed decrease in the critical current.

2.3.2. Static interaction of a vortex lattice with corrugated films in a strong magnetic field

A theoretical analysis of superconducting corrugated films cannot be complete without an examination of behavior of these films in strong magnetic fields ($H_{c2} - H \ll H_{c2}$). This case has been considered by Kuziĭ,[65] who studied a thin film with a rather long wavelength sinusoidal corrugation ($\lambda_g \gg d$). Here, in the Ginzburg–Landau functional (2.9), which is applicable to uniform thin films, it is necessary to replace $g(z)$ by $g(z)K$, where

$$K = 1 + \frac{\Delta d}{d}\cos[\mathbf{q}(\mathbf{r} - \mathbf{r}_0)],$$
$$\mathbf{q} = \frac{2\pi}{\lambda_g}(\cos\theta, \sin\theta) \tag{2.33}$$

and θ is the angle between the vectors $\mathbf{e}_x$ and $\mathbf{q}$. By minimizing the free energy obtained in this way it is easy to find the modified Ginzburg–Landau equations

$$\left(\frac{\partial}{i\varkappa\partial\mathbf{r}} - \mathbf{A}\right)K\left(\frac{\partial}{i\varkappa\partial\mathbf{r}} - \mathbf{A}\right)\psi = K(\psi - |\psi|^2\psi), \tag{2.34}$$

$$\mathrm{curl\,curl}\ \mathbf{A} = \frac{1}{2}g(z)K\left[\psi^*\left(\frac{\partial}{i\varkappa\partial\mathbf{r}} - \mathbf{A}\right)\psi - \psi\left(\frac{\partial}{i\varkappa\partial\mathbf{r}} + \mathbf{A}\right)\psi^*\right]. \tag{2.35}$$

Kuziĭ[65] examined the case of a vortex lattice commensurate with the corrugation. The procedure of the calculation is similar to that for calculations of the analogous functions by Ami and Maki[75] for bulk superconducting alloys with sinusoidally varying concentrations of impurities.

To solve the system of equations (2.34) and (2.35) Ami and Maki used the system of orthogonal functions of Eilenberger,[76] which are defined as follows:

$$\varphi_0(\mathbf{r}) = \left(\frac{2\eta'}{b^2}\right)^{1/4}\exp\left(-\frac{\pi y^2}{\eta'}\right)\vartheta_3\left(\pi\frac{z}{b}\,\middle|\,\frac{\tau}{b^2}\right), \tag{2.36}$$

$$\varphi_n(\mathbf{r}) = \left[\left(\frac{4\pi}{\eta'}\right)^n n!\right]^{-1/2}F_+^n\varphi_0(\mathbf{r}), \tag{2.37}$$

where

$$\mathbf{r} = (x, y),\ \eta' = 2\pi/\varkappa_0 B,\ z = x + iy,\ \tau = \zeta + i\eta',$$
$$F_\pm = i^{-1}\frac{\partial}{\partial x} + \frac{2\pi y}{\eta'} \mp \frac{\partial}{\partial y},$$
$$\vartheta_3(z|\tau) = \sum_{p=-\infty}^{\infty}\exp(2pzi + \pi\tau p^2 i); \tag{2.38}$$

and ϑ_3 is the elliptical theta function of Reimann. The Eilenberger functions are solutions of the equation

$$\left(\frac{\nabla}{i\varkappa_0} - \mathbf{A}_0\right)^2 \varphi_n = \frac{1}{\varkappa_0^2}(F_+F_- + \frac{2\pi}{\eta'})\varphi_n = \varepsilon_n\varphi_n, \tag{2.39a}$$

where $\mathbf{A}_0 = \mathbf{e}_x By$ and

$$\varepsilon_n = \frac{2\pi}{\varkappa_0^2\eta'}(2n+1), \quad n = 0,1,2,...; \tag{2.39b}$$

where $\mathbf{e}_x$ is the unit vector in the direction of the x axis. This equation is formally analogous to the Schrödinger equation for the motion of a particle of charge $2e$ in a static magnetic field B. As any such trial functions in perturbation theory they satisfy the orthogonality condition

$$\int \varphi_n^*\varphi_m^* d^2\mathbf{r} = \delta_{nm}\int d^2\mathbf{r}.$$

The two-dimensional periodic function $\varphi_0(\mathbf{r})$ describing the vortex lattice in the x-y lane has the periods

$$\mathbf{r}_1 = (b,0), \quad \mathbf{r}_2 = b^{-1}(\zeta,\eta'). \tag{2.40}$$

If the small amplitude of the thickness modulation is taken into account the Eilenberger functions for the vortex lattice can be written as

$$\varphi = \varphi_0(\mathbf{r}) + w_1\varphi_1(\mathbf{r}). \tag{2.41}$$

The coefficient w_1 is found from the linearized equation (2.34), having the form

$$\left(\frac{\partial}{i\varkappa\partial\mathbf{r}} - \mathbf{A}_0\right)K\left(\frac{\partial}{i\varkappa\partial\mathbf{r}} - \mathbf{A}_0\right)\psi - \frac{\Delta d}{d}\cos[\mathbf{q}(\mathbf{r}-\mathbf{r}_0)]\psi = E_e\psi. \tag{2.42}$$

Substituting the function (2.41) into this equation, following Ref. 65, we obtain

$$E_e = E_0 - \frac{\Delta d}{d}uQ\cos(\mathbf{qr}), \tag{2.43}$$

where

$$u = (q^2 + 2\varkappa^2 - 2\varkappa H)/2\varkappa^2, \tag{2.44}$$

$$Q = \exp\left(-\frac{q^2}{4\varkappa H}\right)(-1)^{mn} I(-b\cos\theta\cdot a)I\left(\frac{2\pi\sin\theta}{\varkappa Hab} + \frac{\zeta\cos\theta}{ab}\right), \tag{2.45}$$

where $I(x) = 1$ if x is an integer and zero otherwise, and m and n are the integral values x of the function $I(x)$ in expression (2.45). Minimizing E in second order in $\Delta d/d$ we obtain

$$w_1 = -iQ\sin(\mathbf{qr}_0)\frac{\Delta d\cdot qv\exp(i\vartheta)}{d(2\varkappa H)^{1/2}}, \tag{2.46}$$

$$v = (q^2 + 2\varkappa^2 - 4\varkappa H)/4\varkappa H. \tag{2.47}$$

These expressions for E and w_1 differ from the corresponding ones for a bulk layered superconductor only in the coefficients u and v. In the case of a bulk superconductor the term in $\varkappa^2$ is absent in the numerators of these coefficients. This difference is due to the fact that the left-hand side of the linearized equations (2.34); that is, it is due to the fact that the corrugation affects not only the gradient term. As a result, when the vortex lattice is commensurate with the corrugations the free energy is given by

$$F = -\frac{[\varkappa + \varkappa uQ\cos(\mathbf{qr}_0)(\Delta d/d) - H]^2}{\beta_A(2\varkappa^2 - f^*)}. \tag{2.48}$$

The free energy has a minimum when the term $\varkappa uQ\cos(\mathbf{qr}_0)\Delta d/d$ has a maximum and the coefficient β_A has a minimum. As is well known, β_A has a minimum for the triangular lattice and the maximum of the term is equal to $\tau' = \varkappa u\exp(-q^2/4\varkappa H)\Delta d/d$, in which case all the vortices are located at regions of minimum film thickness. If the field is slightly displaced from the matching field, which is defined by relation (2.16), the vortices remain in the regions of minimum thickness, but the lattice is deformed and the coefficient β_A increases.

As usual, the critical current is found from the condition that the maximum pinning force and the Lorentz force be equal. In reduced coordinates this equality is expressed by

$$\nabla_{q_0}F + 2\langle\mathbf{j}_c\rangle\times\mathbf{H} = 0. \tag{2.49}$$

The extra coefficient 2 in the second term is due to the use of reduced coordinates. This condition gives the following value for the critical current

$$j_c = j_{c,m} = \frac{qd}{\beta_A(2\varkappa^2 - f^*)H}\left\{\left[\frac{(\varkappa - H)^2}{16} + \frac{\tau'^2}{2}\right]^{1/2} + \frac{3(\varkappa - H)}{4}\right\}^{3/2} \times\left\{\left[\frac{(\varkappa - H)^2}{16} + \frac{\tau'^2}{2}\right]^{1/2} - \frac{\varkappa - H}{4}\right\}^{1/2}. \tag{2.50}$$

This relation is valid for $H = B_{mn}$. When the critical current is calculated for a magnetic field that is not far from these values, edge effects are important, and taking them into account results in a larger critical current. The following section analyzes this effect.

2.3.3. Dynamic interaction of a vortex lattice with a corrugated film

In the motion of vortices, forces due to their viscous motion act on those vortices in addition to the Lorentz force and the pinning force. The equation of motion of the vortices is derived from the condition of balance of these three forces. For a sinusoidal variation of the film thickness this equation is[71]

$$\eta\partial\mathbf{r}_n/\partial t = \mathbf{F}_n + \mathbf{q}\Delta\varepsilon\sin[\mathbf{q}(\mathbf{r}_n - \mathbf{r}_0)], \tag{2.51}$$

where $\eta\partial r_n/\partial t$ and $\mathbf{F}_n = \mathbf{j}\times\mathbf{\Phi}_0/c$. This equation is like the one for determining the phase difference of the order parameter in the resistive model of the Josephson junction (Section 2.2.1.). Moreover, the rate of change of the phase difference in a superconductor is proportional to the vortex velocity; that is, to find the voltage across the sample one must use an equation analogous to (1.2b). Thus, Eq. (2.51) implies, for example, that the I–V characteristic of a corrugated film in a magnetic field must have the hyperbolic form characteristic of a Josephson junction

$$\langle E(t)\rangle \sim (I^2 - I_c^2)^{1/2}, \tag{2.52}$$

where $\langle E(t)\rangle$ is the constant component of the electric field

on the film. Its alternating component is given by the formula

$$\frac{E(t)}{\langle E\rangle} = 1 + 2\sum_{m=1}^{\infty}\left[\frac{I^2 - (I^2 - I_c^2)^{1/2}}{I_c}\right]^m \cos(m\omega_i t), \qquad (2.53)$$

where $\omega_i = 2\pi c\langle E\rangle/\lambda_g B_{nk}$. If the film is placed in an electromagnetic field with a frequency ω, then, as in the case of Josephson junctions, interference is observed between this field and the intrinsic emission, and steps appear in the I–V characteristics,[69] located at

$$E_n = n\frac{\omega\lambda_g B_{mk}}{2\pi c}. \qquad (2.54)$$

Since, as follows from formula (2.53), the intrinsic radiation has a whole spectrum of harmonics in addition to the fundamental, subharmonic steps should be observed on the I–V characteristics.

2.4. Vortex lattices incommensurate with the corrugations

2.4.1. Vortex lattice incommensurate with the corrugations at zero temperature

Interesting phenomena occur when the vortex lattice is not commensurate with the corrugations. In this case the object of the investigations is in many ways related to a lattice of atoms in a periodic one-dimensional field. The behavior of a vortex lattice in a thin film is governed by two factors: its elasticity and its interaction with the periodic potential of the corrugated film. Since the bulk modulus for a vortex lattice in a thin film is infinite, the transverse shear strain of the vortex lattice plays an important role in this case. For this strain, the elasticity of the lattice is characterized by the following force constant

$$D_t(\mathbf{k}) = K_t k^2, \qquad (2.55)$$

where $K_t = \mu\phi_0/B$ and $\mathbf{k} = \mathbf{q} - \mathbf{g}$. The elastic interaction between vortices in a superconductor results in the formation of a regular triangular lattice. However, when the vortex lattice and the corrugations are not commensurate, their interaction causes a distortion of this lattice.

1) $H \ll H_{c2}$. Unlike the work of Martinoli,[71] where the discrete nature of the vortex lattice was of primary importance, in the work of Pokrovskiĭ and Talapov[77] and of Burkov and Pokrovskiĭ,[78] the properties of a continuous strain field were studied, neglecting the effect of thermal fluctuations. The mismatch δ is defined as

$$\delta = \frac{B - B_{nk}}{2B_{nk}}.$$

Burkov and Pokrovskiĭ[78] have shown that there are critical values of the mismatch δ_{cnk} which separate regions of commensurate and incommensurate phases. In the commensurate phase the long-range order of the vortex lattice is maintained, but for $\delta \neq 0$ the unit cell is deformed. An example of such a deformation in the case of magnetic fields close to B_{10}, the fundamental matching field, is shown in Fig. 11. In the incommensurate phase a soliton structure arises; this phase has regions, large compared to the period of the vortex lattice, in which the vortices are located in the troughs of the corrugations, and these regions alternate with narrow stripes (solitons) in which there are $N \pm 1$ vortices in N periods of the substrate. The solitons are situated at an angle of

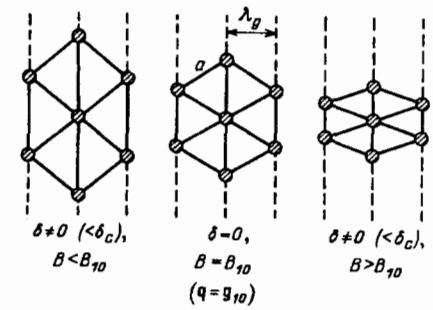

FIG. 11. Changes in the shape of the vortex lattice in the commensurate phase for various values of the mismatch parameter (Ref. 72).

45° to the corrugations. Since in this case the energy of the system is invariant under a translation of the lattice by an arbitrary distance, the phase of the critical current in an incommensurate lattice is zero. In a real situation the defects of the film and the corrugation create additional pinning centers, so that the critical current in the incommensurate phase does not go to zero.

To describe a system of Abrikosov vortices the following Hamiltonian was used in these investigations

$$H = \int [(\mu/2)(\partial x_1/\partial x - \partial y_1/\partial y - 2\delta)^2 + (\mu/2)(\partial x_1/\partial y + \partial y_1/\partial x)^2 + \tilde{V}(x_1)]\,dxdy, \qquad (2.56)$$

where x_1 and y_1 are the components of the displacements of the vortices from their equilibrium positions along the y and x axes in the commensurate phase, and the transport current I is in the direction of the y axis. In the London case, ($\xi_0 \ll \lambda_L$ and $H \ll H_{c2}$) the potential $\tilde{V}(x_1)$ can be written as

$$\tilde{V}(x_1) = \frac{H}{\phi_0}\left[\Delta d(x_1)\left(\frac{\phi_0}{4\pi\lambda_L}\right)^2 \ln\frac{\min(a_0, 2\lambda_\perp)}{\xi} - \frac{j\phi_0 x_1}{c}\right]. \qquad (2.57)$$

Since the bulk modulus of the vortex lattice is infinite, we have $\partial x_1/\partial x + \partial y_1/\partial y = 0$. The commensurate phase in the interior of the sample corresponds to the solution in which all the vortices are located at the minima of the potential $\tilde{V}(x_1)$ (see Fig. 11). However, in a narrow layer near the boundaries of the sample the symmetry of the distribution relative to the corrugations is broken. These vortices are displaced from their equilibrium positions, and if the modulation of the potential $\tilde{V}(x_1)$ is sufficiently small, that is, for a shallow corrugation, the barrier that prevents the generation of solitons vanishes. It is clear that in this case Eq. (2.26) does not apply, and, because of the motion of the solitons a voltage is generated that prevents the ordered motion of the vortex lattice as a whole. The critical current is given by the condition

$$\tilde{V}_{\max} - \tilde{V}_{\min} = 2\mu\delta^2, \qquad (2.58)$$

that is, the critical current is determined mainly by the shear modulus. In corrugated films for $H \ll H_{c2}$ the shear modulus is given by the expression

$$\mu = 1.47\cdot 10^{-3}(\phi_0 H^3)^{1/2} G(a_0/\lambda_\perp), \qquad (2.59)$$

where $G(a_0/\lambda_\perp)$ is a dimensionless function calculated in Ref. 78. If $a_0 \gg \lambda_\perp$, then $G = 4.2$, and in the other limit (where $a_0 \ll \lambda_\perp$), $G = a_0/\lambda_\perp$. Substituting this relation into

Eq. (2.58) we can determine the dependence of the critical field on the initial mismatch

$$\left(\frac{\Delta d(x_1)\phi_0}{8\pi\lambda_g\lambda_L^2}\ln\frac{\min(a_0,2\lambda_\perp)}{\xi}-\frac{j_c dx}{c}\right)_{\max}-\left(\frac{\Delta d(x_1)\phi_0}{8\pi\lambda_g\lambda_L^2}\ln\frac{\min(a_0,2\lambda_\perp)}{\xi}-\frac{j_c dx}{c}\right)_{\min}=\delta^2\frac{H}{16\pi}G(a_0/2\lambda_\perp). \quad (2.60)$$

A plot of $j_c(H)$, calculated from relation (2.60) for the region of the commensurate phase is shown in Fig. 12. As can be seen, if the boundary phenomena are taken into consideration we obtain a smooth variation of $j_c(H)$. If the creation of solitons at the boundary between the commensurate and incommensurate phases is not taken into account, that is, if $\delta=\delta_{cnk}$, one would observe a sharp falloff of the critical current to zero. Another interesting phenomenon has been predicted in Ref. 78. Near the maximum possible mismatch δ_{cl} calculated in this paper, one ought to see a region of instability of the vortex lattice in the commensurate phase. In a certain range of variation of the mismatch parameter $\delta_c<\delta<\delta_{cl}$ the commensurate phase is found to be metastable. Since $j_c=0$ in the incommensurate phase, the critical current depends on the initial phase of the vortex lattice, that is, hysteresis is possible.

2) $H_{c2}-H\ll H$. The edge effect of matching also has a large effect on the magnitude of the critical current in strong magnetic fields.[65] In Ref. 65 the same Hamiltonian was used for the calculation, and the dependences of the critical current on the magnetic field came out to be similar to the dependences $j_c(H)$ for weak magnetic fields.

2.4.2. Mismatch of the vortex lattice with the corrugation at a finite temperature

It is well known[66] that in thin superconducting films thermal fluctuations have a strong effect on the vortex lattice, softening it, and even melting it near T_c. Therefore, in corrugated films the behavior of a vortex lattice at finite temperatures must be quite different from that at zero temperature. The transition from the incommensurate to the commensurate phase of the vortex lattice at a finite temperature

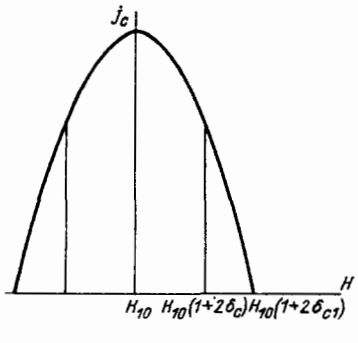

FIG. 12. Curve of $j_c(H)$ for the commensurate phase near B_{10} (Ref. 78).

has been studied in Ref. 72. Following this work, let us consider the case of complete matching $\delta=0$, which is particularly simple. Under the action of thermal fluctuations the vortices undergo Brownian motion about their zero-temperature equilibrium positions. The equation of motion of a vortex with the coordinates $\mathbf{r}_{1l}$ can be written as

$$\eta\partial\mathbf{r}_{1l}/\partial t+\mathbf{q}l\varepsilon\sin(\mathbf{q}\mathbf{r}_{1l})+\sum_{\substack{l'\\(l\neq l')}}\tilde{G}(l-l')\mathbf{r}_{1l}-\mathbf{F}_{Ll}(t)=0. \quad (2.61)$$

In this equation, two new terms appear in addition to the usual terms describing the vortex lattice; these are $\tilde{G}(l-l')$, the matrix of the elastic interaction between the vortices in the lattice, and $F_L(t)$, the Langevin force, which satisfies the relation

$$\langle F_{Ll}^{\alpha}(t)F_{Ll'}^{\beta}(t)\rangle=2\eta k_B T\delta_{\alpha\beta}\delta_{ll'}\delta(t-t'). \quad (2.62)$$

Equation (2.62) is solved by the usual procedure of transforming to **k**-space:

$$\mathbf{r}_{1l}(t)=\frac{1}{2\pi}\int_{-\infty}^{+\infty}\sum_{k,p}r_{1k}(\omega)\mathbf{e}_{kp}\exp[i(\mathbf{k}\mathbf{l}-\omega t)]d\omega, \quad (2.63)$$

where $\mathbf{r}_{1k}(\omega)$ are the amplitudes of the normal modes and $\mathbf{e}_{kp}$ are unit vectors for the longitudinal ($p=l$) and the transverse ($p=t$) strains in the vortex lattice. Linearizing equation (2.61) and taking into account only the transverse modes of oscillation of the vortex lattice, we obtain

$$r_{1kt}(\omega)=\frac{F_{Lkt}(\omega)}{D_{kt}+\Delta\varepsilon_R(\mathbf{q}\mathbf{e}_{kt})^2-i\eta\omega}, \quad (2.64)$$

where D_{kt} is an element of the diagonalized matrix of the elastic interactions related to the transverse modes of oscillation of the vortex lattice, and $F_{Lkt}(\omega)$ is the transverse Fourier component of the Langevin force. The fluctuation-induced motion of the vortices about the equilibrium positions causes a decrease in the effective value of the periodic pinning potential ($\Delta\varepsilon_R$), which in turn causes the matching of the vortex lattice with the corrugations when $\delta\neq0$. The decrease $\Delta\varepsilon_R$ causes a logarithmic increase in the mean square deviation of the vortices from their equilibrium positions. The temperature dependence of $\Delta\varepsilon_R$ has been calculated in Ref. 72. In the case of a shallow corrugation, where $\Delta\varepsilon\ll\mu\lambda_R^2$,

$$\frac{\Delta\varepsilon_R}{\Delta\varepsilon}=\left(\frac{\Delta\varepsilon}{\mu}\right)^{T/(T_{lu}-T)}, \quad (2.65)$$

where T_{lu} is the temperature of the phase transition of the vortex lattice from the commensurate to the incommensurate phase. Its value at $B=B_{10}$ is given by

$$T_{lu}=T_c\left(1-0{,}31\frac{R_\square e^2}{\hbar}\right), \quad (2.66)$$

where $R_\square$ is the resistance per square of the film. Close to the phase transition, that is, for $T\to T_{lu}$, the effective potential tends to zero and the vortex lattice becomes unstable.

For an experimental check of these results Martinoli *et*

TABLE II.

Film	d, Å	$\Delta d/d$	λ_g, μm	$R_\square$, Ω	T_c, K	$(\xi_0 l)^{1/2}$, Å	$\lambda_L(0)\left(\frac{\xi_0}{l}\right)^{1/2}$, Å
Al1	200	~0.2	0.79	15	1,89	365	4300
Al2	200	~0.2	0.77	35	2,16	223	6140

al.[72] have studied the function $I_c(T)$ for corrugated aluminum films at temperatures close to the critical temperature. The samples were prepared by holographic photolithography. Their characteristic dimensions are listed in Table II. Since the critical current depends on the effective pinning potential (2.65), for $B = B_{10}$ and the usual sinusoidal corrugation (2.18) the following formula can be used for the temperature dependence of the critical current:

$$\frac{I_{c,m}(T)}{I_{c,m}(0)} = \frac{\lambda_\perp(0)}{\lambda_\perp(T)}\left(\frac{\Delta\varepsilon}{\mu}\right)^{T/(T_{lu}-T)}. \tag{2.67}$$

For comparison, if the interaction of the thermal fluctuations is neglected, then we obtain the usual dependence

$$I_{c,m}(T) = \frac{I_{c,m}(0)\lambda_\perp(0)}{\lambda_\perp(T)}. \tag{2.68}$$

It follows from formula (2.68) that with an increase in the temperature $T \to T_{lu}$ the smearing of the pinning potential by the thermal fluctuations causes a sharp decrease in the critical current $I_{c,m}(T)$ to zero. The experimental curve of $I_{c,m}(T)$ obtained by these workers (Fig. 13) supports the correctness of this formula. The solid lines on this figure show the curves given by expression (2.67), and the dashed lines represent the function (2.68). The agreement between theory and experiment confirms the validity of this method of taking into account the effect of fluctuations on the vortex lattice in corrugated superconducting films.

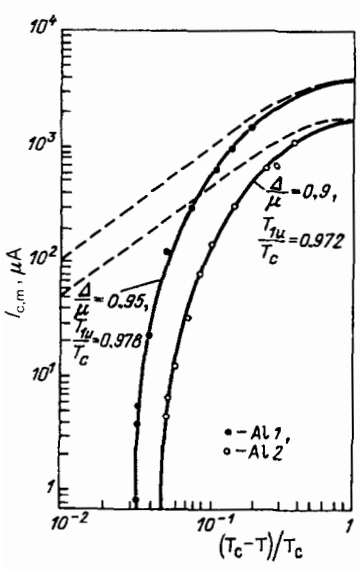

FIG. 13. Temperature dependence of the critical current of a corrugated superconducting film at $B = B_{10}$ (Ref. 72).

2.5. Chains of channels in superconducting films

An interesting method of using superconducting microstructures for the study of the mixed state has been applied in Ref. 79. This paper studied superconducting two-layer films containing a chain of narrow channels with weak pinning. Figure 14 shows schematically these structures (Fig. 14a is a view from the top and 14b is the transverse cross section). These structures consist of NbN layers separated by narrow channels of $Nb_{0.66}Ge_{0.34}$. Because of their granularity, the NbN films contain a very large number of elementary pinning forces. In amorphous $Nb_{0.66}Ge_{0.34}$ films, on the other hand, the pinning forces are small. This chain contained 200 individual channels. To avoid bending of the vortex filaments fairly thin layers of superconductor were used. Since vortices passing through the NbN layers are strongly pinned, the dynamic resistance of the samples in the mixed state studied in this investigation was governed by the motion of vortices in the $Nb_{0.66}Ge_{0.34}$ channels. Because the critical current of the samples is determined by the interaction of the vortices in the channels with the immobile vortices passing through the NbN layers, one can expect that the motion of the vortices in all the channels commences simultaneously. Using these structures allowed Pruijboom *et al.*[79] to measure the resistivity of the samples in the mixed state as a function of the external magnetic field. The investigations showed that the bulk pinning force in these structures obeys the following relation

$$P_v = 0.094\mu/w_c, \tag{2.69}$$

where w_c is the width of the $Nb_{0.66}Ge_{0.34}$ channel. The curve obtained is close to the theoretical one calculated in Refs. 80 and 81 on the assumption of collective pinning.

The coherent motion of Abrikosov vortices at a high velocity in wide and relatively short bridge contacts suggests

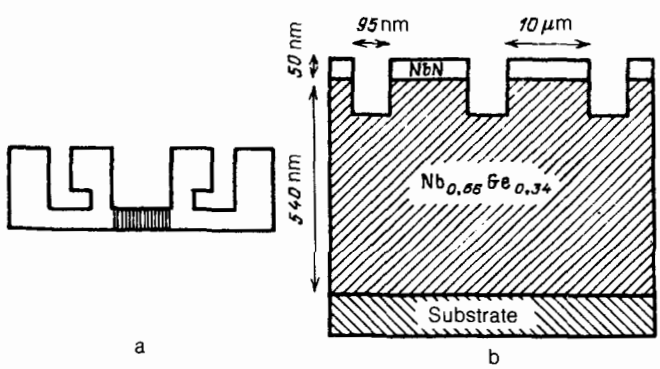

FIG. 14. a) View from the top of the two-layer structure from Ref. 79; b) transverse cross section of the same structure.

the possibility of the same motion of the entire collection of vortices in corrugated superconductor films. When the transport current flows perpendicularly to the corrugations these films can be represented as a chain of series-connected wide bridge contacts of variable thickness. In these structures all the vortices in a chain must move. Moreover, the interaction of the vortices in adjacent chains can result in an ordered motion of all the vortices. This idea was advanced in Ref. 82, and has been confirmed experimentally. The corrugated tin films used in this work were prepared by electron-beam lithography with the use of a positive resist and subsequent plasma-chemical etching of the previously deposited tin film. The film thickness was from 1000 to 2000 Å. The region containing the corrugations was prepared in the form of bridges, whose length and width were 10 μm. This work studied the nature of the action of microwave radiation on these structures. Figure 15 shows I–V characteristics in a microwave field of the same power but with different magnetic fields. As can be seen from this figure, in fields close to the matching field, that is for $B = B_{10}$, the I–V characteristics of the contacts have stepped features at the voltages

$$V_n = 5n\hbar\omega/e. \tag{2.70}$$

The existence of current steps is evidence for the synchronous motion of the vortices over the entire contact; that is, ordered motion is obtained in all 10 rows of vortices. For the formation of the nth current step on an I–V characteristic it is necessary that the frequency at which the vortices enter the film be equal to $n\omega/2\pi$. In a time equal to the period of the radiation the vortex lattice must shift by a distance $2\lambda_g/\sqrt{3}$, so that the velocity of the vortices reaches at least $3\cdot 10^5$ cm/s.

This idea may prove to be helpful for the purpose of developing generators of electromagnetic radiation based on superconducting structures. Figure 16, taken from Ref. 83, shows schematically a structure of this type. The superconducting film has a double corrugation of the same period. The superconducting film has a double corrugation of the same period. The transverse dark lines correspond to the deeper grooves, and the other lines, arranged at an angle of 60° to the former, are the shallower grooves. If a current

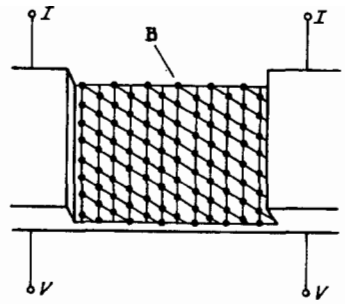

FIG. 16. Thin film structure with a double corrugation in a magnetic field (Ref. 83).

greater than the critical current passes through this film then the Abrikosov vortices in a field equal to B_m will move along the deep grooves. In the special case where the shallower grooves have a sinusoidal profile an electric field with a strength given by relation (2.53) should be set up in the sample. To decrease the effect of randomly situated pinning centers it is better to make the transverse channels of a normal metal. In this case the superconductivity in the structure is maintained by the proximity effect.

2.6. Films with an ordered lattice of holes

This section will deal with the interaction of a vortex lattice with another periodic thin-film structure, a triangular lattice of holes. This problem was first addressed in a paper by Fiory, Hebard, and Somekh.[84] The lattice of holes was prepared by electron lithography. The thin film structure had the following parameters: hole diameter 0.5 μm, spacing between holes 3 μm, and thickness of superconducting film 0.1 μm. As usual, the films used were of granular aluminum, deposited in an oxygen atmosphere. The critical current was observed to depend nonmonotonically on the magnetic field (Fig. 17). The more pronounced peaks on the curve of $I_c(B)$ were observed at $B = nB_m$, where the matching field B_m is found from the usual geometric considerations:

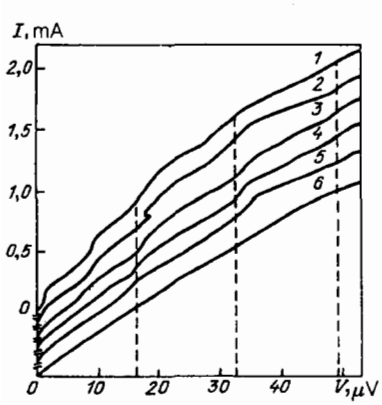

FIG. 15. I–V characteristics of corrugated superconducting films in a microwave field of frequency 800 MHz, with the same power for the curves but different magnetic fields (in Gauss): *1*) 17; *2*) 17.4; *3*) 17.8; *4*) 18; *5*) 18.2; *6*) 18.6 (Ref. 82).

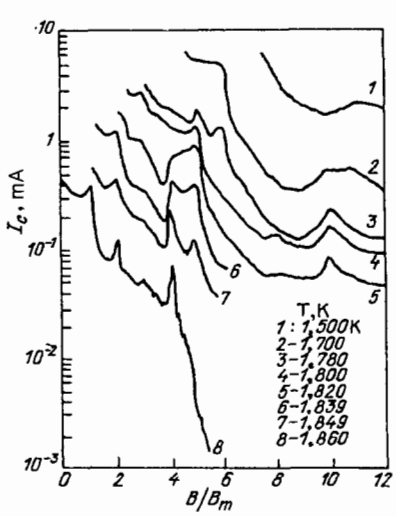

FIG. 17. Critical current in a film with a lattice of holes as a function of the magnetic field for various temperatures (Ref. 84).

$$B_m = 2\phi_0/\sqrt{3}a_h^2; \quad (2.71)$$

where a_h is the spacing between the holes. The authors assumed that in the film containing the holes a magnetic field equal to a multiple of B_m forms a coupled bunch of n vortices near each hole. The interaction potential between the vortices and a cylindrical hole of radius r_h has been determined in Ref. 85 and is given by

$$U = (\phi_0/4\pi\lambda)^2 d \ln(2r_h/\xi). \quad (2.72)$$

It can be seen that these holes can be effective pinning centers in superconducting films.

There are two possible ways of explaining this phenomenon. In the first, it is assumed that the holes are shallow, that is, the pinning force is small compared to the elastic forces of the vortex lattice. In this case one can use the results of Martinoli[71] for the explanation of similar curves in the case of corrugated films. When the vortex lattice matches the lattice of inhomogeneities in the film there is a minimum in the free energy, which also leads to a maximum in the curve of $I_c(B)$.

An interesting approach to the analysis of $I_c(B)$ in these structures has been proposed by Blamire.[86] He regarded the holes as having a fairly high pinning potential compared to the elastic interaction of the vortices. Figure 18 shows the occupation of the holes by vortices in two cases: a) B is slightly larger than B_m; b) B is slightly less than $2B_m$. In the former case a single vortex is found in almost every hole, but there are a small number of holes (Fig. 18a) which contain one additional vortex. In the latter case, conversely, almost all the holes contain just two vortices, while a small number of them contain only one (Fig. 18b). An analysis of the forces[87,88] shows that the extra vortices (case a) or the vortices located near a vacancy (case b) are acted on by an additional force approximately equal to the force of repulsion of the vortices (case a) either in the holes or located nearby (case b). Therefore, these extra or deficient vortices can more easily than the rest of the vortices move under the action of the Lorentz force. It is clear that the voltage across the sample is given by

$$V = N_v \phi_0 \langle v \rangle l_m, \quad (2.73)$$

where $N_v = |B - nB_m|/\phi_0$ defines the degree of mismatch between the vortex lattice and the hole lattice, n is an integer, and $\langle v \rangle$ is the average velocity of the vortices. Since the Lorentz force on a vortex is proportional to the current, the velocity $\langle v \rangle$ increases monotonically with the current. Experimentally, the critical current is defined as that value of the transport current passing through the sample for which the voltage across the sample attains a certain small value. near nB_m, where a small number of excess or deficient vortices are present in the film, it is necessary that a large current pass through the bridge to cause these vortices to move sufficiently fast, according to relation (2.73). At this field a peak should appear on the curve of $I_c(B)$, and a graph of the current at which the vortices can leave the potential wells of the holes and start moving, plotted as a function of the magnetic field, exhibits steps: the current falls off smoothly as the magnetic field increases, and then for $B \geqslant nB_m$ it has a sharp dropoff. This behavior occurs because it is easier to set into motion the excess vortices than the deficient vortices when the vortex lattice and the hole lattice are perfectly matched. On the basis of these arguments, Blamire[86] calculated $I_c(B)$, the curve of which is shown in Fig. 19. It can be seen that there is good agreement between this theoretical curve and the experimental curve obtained by Fiory and his coworkers.[84]

Fiory *et al.*[84] used granular aluminum films in which the pinning is extremely weak. The work reported in Refs. 89 and 90 was focused on the influence of lattice matching in porous films with rather strong pinning. The lattice of holes was prepared by means of electron beam lithography with a positive resist and plasmachemical etching of the previously deposited tin film. The film thickness ranged from 300 to 2000 Å. The unit cell was an isosceles triangle with a height and base of length either 0.8 or 1.0 μm. The tin films that were used had a critical current and a pinning force considerably larger than in the granular aluminum films. In these experiments a shift was observed in the peaks as functions of nB_m, where the position of the peaks depended on the way the magnetic field varied. In an increasing magnetic field the peaks shifted towards lower magnetic fields relative to nB_m, and, conversely, in a decreasing magnetic field they shifted towards higher fields. The amount of the shift increased with a reduction in the temperature and in the integer n. If the sample was heated above T_c prior to each measurement, then the peaks were observed near nB_m (Fig. 20). This behavior was explained by invoking the magnetic field gradient

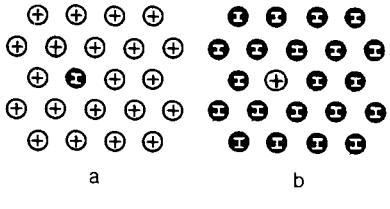

FIG. 18. Schematic representations of two cases of quantized vortices filling a film with a hole lattice. a) Extra vortex in a lattice of holes each filled with just one vortex; b) a vortex vacancy in the lattice of holes, each containing two vortices (Ref. 86).

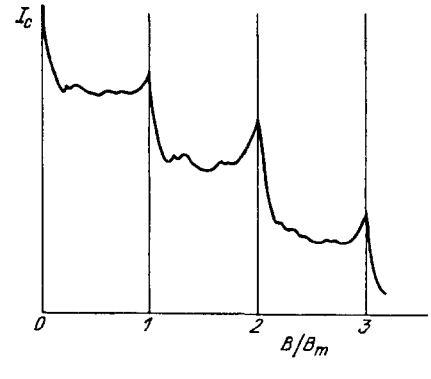

FIG. 19. Variation of the critical current determined for a constant voltage level, calculated in Ref. 86.

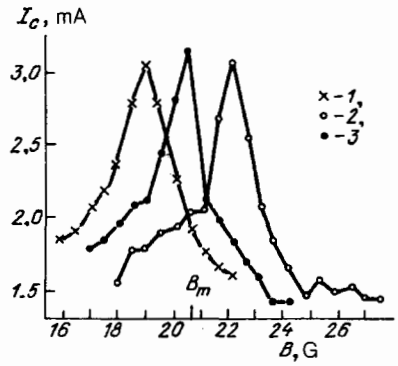

FIG. 20. Dependence of the critical current on the external magnetic field strength for a lattice of superconducting thin-film holes at $T = 3.33$ K. *1)* Increasing field; *2)* decreasing field; *3)* variation of the field with the sample temperature above T_c (Ref. 90).

that arises in the plane of a sample with strong pinning centers. In an increasing magnetic field the vortex density at the edges of the film is greater than in the center, and conversely, in a decreasing field the density at the edges is smaller. Because of this gradient the vortices move as required to establish the equilibrium mixed state. Since the current density in wide films is higher at the edges that in the center, the critical current is determined mainly by the interaction of the vortices with the pinning centers at the edges of the film. If the vortex lattice at the edges of the film matches the hole lattice a peak should appear on the curve of $I_c(B)$, a conclusion which also explains the observed hysteresis in $I_c(B)$. The interaction of the vortices with the pinning centers falls off with increasing temperature, which should lead to a decrease in the hysteresis. In addition, the mutual repulsion of the vortices also reduces this interaction as n increases, so that the shifts in the peak positions should also be reduced. In this way, the magnetic field gradient can prevent matching of the vortex lattice with the hole lattice. This matching should be observed if the sample is cooled in the magnetic field.

Measurements have also been carried out[90,91] on the temperature dependence of the upper critical field of superconducting films with a lattice of microscopic holes. An example of such a dependence is shown in Fig. 21. This figure shows that this dependence differs considerably from the straight line $H_{c2}^{\perp} \sim T - T_c$ valid for ordinary superconducting films. Structure appears on the background of a square root dependence $H_{c2}^{\perp} \sim (T - T_c)^{0.5}$ when the magnetic field is a multiple of the matching field B_m. This structure appears because the superconducting order parameter is suppressed by the magnetic field to a lesser extent than when the vortex centers are situated in the holes, i.e., when $B = nB_m$. The square root dependence of the upper critical field is characteristic of the upper critical field in the parallel direction for thin films $[d < \xi(T)]$. Therefore, the square root dependence $H_{c2}^{\perp} \sim (T - T_c)^{0.5}$ is evidence that the hole walls are much thinner than the coherence length.

Measurement of the critical current in a static magnetic field $B = B_m$ provides information on the elementary pinning forces. It has been observed[90] that when $B = B_m$ the dependence of the critical field on the temperature far from T_c, where $\xi(T) < 2r_h$, goes as $I_c(T) \sim (T - T_c)^{1.5}$. As T_c is approached there is a sharp decrease in I_c. This type of behavior is easy to explain: If the hole diameter in the film is greater than the coherence length, then the relation $f_p \approx \xi H_c^2/8 \sim (T - T_c)^{1.5}$ holds for the elementary pinning force, which determines the critical field.

An interesting problem of superconductor microelectronics is the development of memory cells based on Abrikosov vortices. In any cell based on such a film there must be two stable states: with and without a vortex. The speed of the vortices in these structures and the energy released in this motion determine the speed of information processing and the packing density of the elements. Desirable materials for memory cells are films with the highest possible vortex velocity and the lowest possible coefficient of viscosity. Possible schemes of generating single vortices and detecting them have been published in Ref. 92. Furthermore, for the operation of these devices it is necessary to have films with little random pinning.

A model of a memory based on a superconducting film with a hole lattice has been proposed by Hebard and Fiory.[93] An important element of this scheme is a system of narrow films that control the arrangement of the vortices. A sketch of this structure and a cross section in one of the directions are shown in Figs. 22 and 23. The external magnetic field applied to this structure is determined by the condition, Eq.

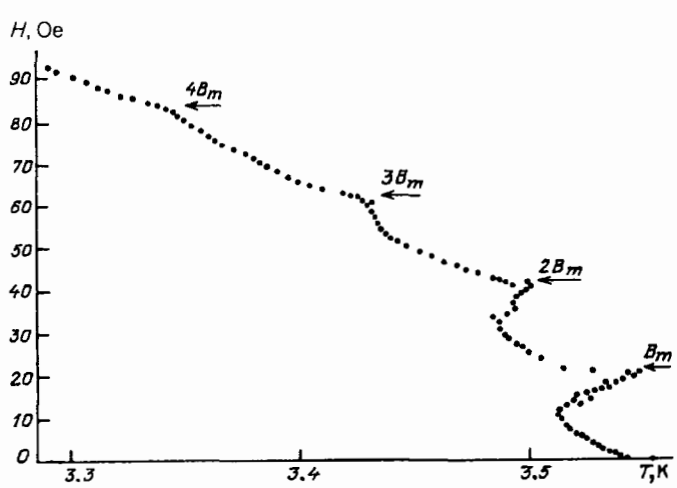

FIG. 21. Temperature dependence of the upper critical magnetic field of a 600 Å tin film with a hole lattice (Ref. 90).

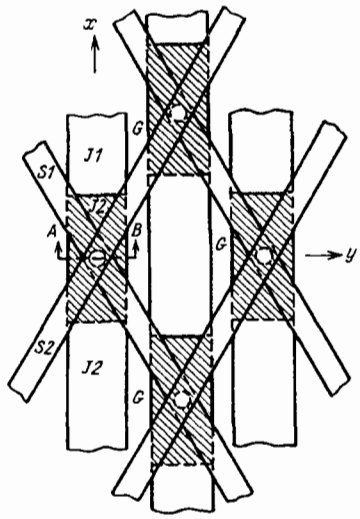

FIG. 22. Memory cell based on a superconducting film with a hole lattice (Ref. 93).

(2.71), of matching the vortex lattice with the hole lattice. The processing of information is accomplished by the motion of the vortices into positions above the holes in the films. The main elements of this structure are the Josephson junctions with the electrodes J1 and J2. These junctions are located above the holes. Above each junction there is a pair of insulated superconducting films S1 and S2. To write a unit of information in any cell it is necessary to move a vortex from location A to location B. This is done by passing a current pulse simultaneously through films S1 and S2. The expected switching time for a contact with a small capacitance should be of the order of 10^{-12} s. The energy dissipated in a switching cycle depends on the critical current of the Josephson junctions and may be of the order of $5\cdot 10^{-10}$ ergs.

3. PINNING IN LAYERED SUPERCONDUCTING STRUCTURES

3.1. Introduction

In layered superconducting structures the superconductor layers alternate with other layers, either of another superconductor (S/S′), a normal (non-superconducting) metal (S/N), a semiconductor (S/s), or an insulator (S/I). The study of the equilibrium properties of artificial layered

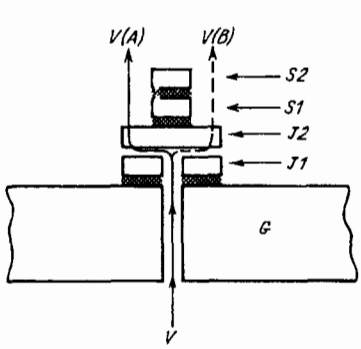

FIG. 23. Transverse view of Fig. 22. $V(A)$ and $V(B)$ show the two equivalent positions of the quantized vortex in the structure, corresponding to "0" and "1" (Ref. 93).

structures is the subject of a review by Jin and Ketterson.[94] The most interesting effect along these lines is the two-dimensional (2D) to three-dimensional (3D) transition. This transition involves the following. If the period λ_s of the layered structure is not much greater than the coherence length $\xi_z(0)$ in the direction perpendicular to the layers, then there is a temperature T' such that if $T'<T<T_c$, then $\xi_z(T)>\lambda_s$, while if $T<T'$, then $\xi_z(T)<\lambda_s$. Near T_c the parallel critical magnetic field varies linearly with the temperature $H^{\parallel}_{c2}(T)\sim T_c-T$; that is, the layered structure behaves as a three-dimensional superconductor. At low temperatures, where $T<T'$, the parallel critical field obeys a square root dependence

$$H^{\parallel}_{c2}(T)=-\frac{2\sqrt{3}\phi_0}{2\pi\xi_z d_l}\sim(T_c-T)^{1/2}, \tag{3.1}$$

which is characteristic of thin $[d\ll\xi(T)]$ superconducting films.[95] This phenomenon is due to deformations of the vortex core in layered superconductors, for which the cross section is determined by two quantities $\xi_z(T)$ and $\xi(T)$. For small $\xi_z(T)$ the vortices can be located in the space between the superconducting layers, and consequently they no longer contribute to the depairing of the superconducting current carriers. In this case the vortices are similar to Josephson vortices.

Since the discovery of the high-T_c superconductors there has been renewed interest in the effect of fluctuations on the properties of layered superconductors. As is known,[96] in a purely two-dimensional superconductor the fluctuations in the phase destroy the long-range order, which is restored when there is even a very small coupling between the layers.[97] A magnetic field parallel to the layers by weakening the interaction between them, increases the role of the fluctuations. In this process an important role is played by the details of the vortex structure in the layered superconductors. In the case of a large anisotropy, when $\xi_z(T)$ is small, the thermal fluctuations easily destabilize the vortex lattice, and the kinks that are formed in the vortices because of their tendency to be located between the layers destroys the long-range order of the vortex lattice even in a perpendicular external magnetic field.[98] In the case of strong thermal fluctuations the formation of new vortices is possible in the individual layers (this is the well-known Kosterlitz–Thouless mechanism) and vortex rings (fluxons) can form in the interlayers between the layers. In principle, these fluxons must weaken the interaction between the superconducting layers. The appearance of two-dimensional superconductivity in this case prevents the fluctuation-induced formation of vortices in these layers. It has been shown[99,100] that the temperature at which the two-dimensional superconductivity is destroyed in layered superconductors as a result of this process is usually above the 3D–2D transition. Nevertheless, the formation of fluxons has a large effect on $H^{\parallel}_{c2}(T)$ (Ref. 100), leading to the formation of a series of step-like structures in it. The magnetic field, penetrating between the superconducting layers, splits them into groups because of the matching effect and weakens the interaction between these groups. As a consequence, 2D superconductivity can arise in these groups of layers. In the range of magnetic fields given by the condition $n(H)\leqslant 8$, where n is the number of super-

conducting layers in the 2D layer (this number, of course, increases with decreasing magnetic field), structure appears because of the fluctuation-induced generation of vortices. This is a consequence of the fact that in strong magnetic fields the temperature at which the two-dimensional superconductivity is destroyed is above the temperature of the 3D–2D transition. The presence of the structure on the curve of $H_{c2}^{\parallel}(T)$ in the range of magnetic fields defined by the condition $n_c \leqslant n(H) \leqslant 9$ is related to the formation of the 2D phase, where the upper limit to the number of layers n_c separating the fluxon chains is determined by the temperature at which the superconductivity is destroyed by the fluxon mechanism. A test of this hypothesis requires layered structures having thin superconducting layers (~ 10 Å) with a relatively large distance between them.

On the other hand, the study of the mixed state and pinning in layered superconducting structures has not as yet received adequate attention. For randomly distributed inhomogeneities the procedure for finding the bulk pinning force P_v depends on the magnetic field strength and the type, the size, and the density of the defects. The problem is complicated by the large density of vortices in ordinary magnetic fields. For example, for $B = 1$ T there are $5 \cdot 10^{10}$ vortices per cm^2. In this context, the ordered superconducting microstructures are a suitable object of investigation. To simplify the procedure of summing up the elementary pinning forces, f_p, one should have strict periodicity in the properties of these structures in space. As mentioned above, in the case of matching of the vortex lattice with the defect lattice one can neglect the elastic properties of the vortex lattice, so that the bulk pinning force is determined by a simple summation of the elementary pinning forces;

$$\mathbf{P}_v = kB\mathbf{f}_p/\phi_0, \tag{3.2}$$

where k is the number of pinning centers in the superconductor per unit length of the vortex filament. At the same time, for the bulk pinning force the following simple expression is valid[101]

$$\mathbf{P}_v = \mathbf{j}_c \times \mathbf{B}, \tag{3.3a}$$

and allows one easily to find $\mathbf{P}_v$ experimentally. Usually, the transport current flows perpendicularly to the magnetic field, and thus the vector equation (3.3a) becomes a scalar equation

$$P_v = j_c B. \tag{3.3b}$$

It follows from relation (3.2), therefore, that in the case of matching of the vortex lattice with the ordered defect lattice the elementary pinning force can be determined experimentally. Such experiments are important, since there are a large number of problems involved with pinning, especially if one has in mind not simply qualitative dependences and effects, but quantitative ones. The use of superconductors with an ordered lattice of inhomogeneities therefore permits a deeper study of pinning.

Unlike planar structures, where the dimensions are presently limited to $\sim 10^3$ Å, it is possible by layer-by-layer deposition to prepare superconducting structures with a period of ~ 10 Å and even less. Moreover, these structures are of interest from the applied point of view. For example, as follows from relation (3.1), the parallel critical magnetic field $H_{c2}^{\parallel}$ in them may be considerably higher than the upper critical field in bulk superconductors.

3.2. Experiment

The first studies of pinning in layered superconducting structures were by Raffy and his coworkers,[102–104] using layered films based on a Pb–Bi alloy. The films were prepared by deposition in a vacuum from separate sources with two electron guns. The deposition rate of the Pb was maintained constant and that of the Bi was varied sinusoidally in time. The resulting concentration of Bi (C_{imp}) in the films varied in thickness along the x axis also sinusoidally with a period of from 700 to 8000 Å:

$$C_{imp}(r) = C_0[1 + \Gamma \sin(2\pi x)\lambda_s^{-1}]. \tag{3.4}$$

The critical current that flows along the layers decreases monotonically in the direction perpendicular to the layers with increasing magnetic field. It is a completely different situation in a parallel field. Figure 24 shows the curves of the critical current as a function of the magnetic field for samples with different modulation amplitudes Γ but with the same period $\lambda_s = 2000$ Å. The most important feature in comparison with a homogeneous sample obtained by annealing the layered sample is that the critical current is considerably higher in layered samples, and it increases with the modulation amplitude. Moreover the function $J_c(H)$ has a maximum whose position depends mainly on the modulation period and on the temperature. As the modulation period decreases, the maximum in $J_c(H)$ shifts towards higher fields. Its position is not determined by the matching field, i.e., it is not equal to B_{10}, where the matching field for layered samples is determined by the usual geometric relation similar to (2.16) for corrugated structures. Instead of the period of the corrugated structures λ_g one must use the period of the layered structures.[103] In addition, as the temperature is increased the maximum shifts towards lower fields, and beginning with the temperature at which the co-

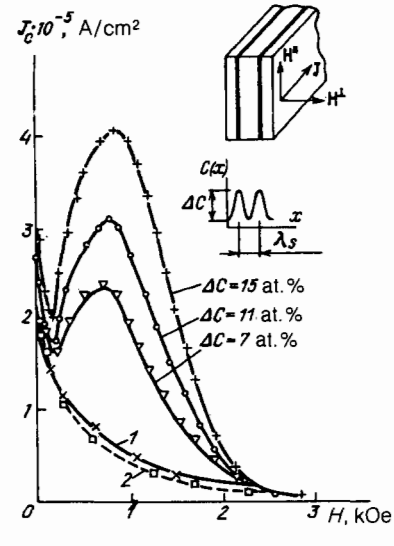

FIG. 24. $J_c(H)$ for layered samples with different amplitudes of modulation of the Bi impurity concentration, with the modulation period 2000 Å; Ref. 102. *1*) Annealed sample; *2*) Homogeneous sample.

herence length is equal to the half period of the layered structure it vanishes.[104] This behavior is evidence for the core mechanism of elementary pinning in these structures.

Some recent publications have dealt with the experimental investigation of the pinning force in layered structures.[105–112] Unlike the work of Raffy and his coworkers, a great deal of attention was paid in these studies to structures based on refractory metals and their compounds, with a tendency to use interlayers that would be effective pinning centers. The most interesting of the results obtained are discussed below.

Broussard and Geballe[105] studied Nb–Ta layered structures. The samples were prepared by magnetron deposition. They used two targets, niobium and tantalum, separated in space. The sapphire substrate was heated during the deposition. Two sets of these structures were studied. In one, identical and fairly thick titanium interlayers (500 Å) were used, with the thickness of the niobium layers varying from 98 to 490 Å. The second set of samples, all had the same ratio of the thickness of the individual niobium and tantalum layers, but different periods λ_s. The most interesting result of this work was the lack of scaling of the pinning force with a change in the operating temperature. A similar phenomenon has been observed by Raffy and his coworkers.[104]

Vermeer *et al.*[106] have studied the angular dependence of the critical current of the layered structures Mo/V and Nb/Pd, with J_c being determined by the magnetic moment, which in turn was determined by measurements of the torque N_t. This method is based on the dependence on the critical current of the gradient of the magnetic induction of the field captured by the superconducting sample. This critical current density is given by the relation

$$J_c(B) = 3N_t/(V_s R_s \cos\theta), \tag{3.5}$$

where θ is the angle between the direction of the magnetic field and the sample surface, and V_s and R_s are the volume and radius of the sample. The samples were prepared by magnetron deposition in an ultrahigh vacuum apparatus. The Nb and Pd layers were of equal thickness, 170 Å. The Mo/V samples had a more complicated structure; each period consisted of two V layers 196 Å thick separated by a thinner 101-Å V layer, and each of these layers was covered by a thin (50 Å) molybdenum interlayer. A large anisotropy of the pinning force was observed: $F_p^{\parallel}/F_p^{\perp} = 30$ at $B = 0.15$ T.

Interesting results were obtained in a study of Nb/NbTi layered structures.[107] The period of the layered structure of the samples was 500 Å. In this investigation Antognazza *et al.* used measurements of $I_c(H,T)$ to obtain additional information on the magnetic phase transition. In the work of Takahashi and Tachiki[113] it was predicted that $H_{c2}^{\parallel}(T)$ for layered samples consisting of alternating layers with identical critical temperatures but with different diffusion coefficients should have a sharp break at a certain temperature T^*. This break in the curve of $H_{c2}^{\parallel}(T)$ arises because when $T < T^*$ the wave function of the superconducting current carriers is localized in the layers with the smaller diffusion coefficient, which contains, for example, a larger number of impurities, while for $T > T^*$ it is localized in the layers with the larger diffusion coefficient. As a consequence, $|\partial H_{c2}^{\parallel}\partial T|$ is considerably smaller at high temperatures than at low temperatures. This behavior of $H_{c2}^{\parallel}(T)$ has been observed in layered structures.[114] In the work of Antognazza *et al.*[107] it was found that the shift of the nucleation of the superconducting phase from the dirty to the clean layers produces structure on the curve of $I_c(T)$ in a field parallel to the layers. Figure 25 shows examples of these curves for various temperatures. The critical current was determined from the I–V characteristics. When the temperature is above T^* superconductivity appears only in the niobium layers and the curve of $I_c(H)$ has no structure. At low temperatures a break appears in this curve at $H = 30.5$ kG. This is consistent with the nature of the dependence $H_{c2}^{\parallel}(T)$, which also was determined in that investigation. At $T = 4.3$ K a break appeared in the diagram just at $H = 30.5$ kG. For $H < 30.5$ kG the maximum of the order parameter lay in the niobium layers and at high fields in the NbTi layers.

To obtain more effective pinning centers, Yetter *et al.*[108] used thin (20 Å) interlayers of the antiferromagnetic metal chromium. The superconducting layers were of a Pb-18 Å Bi alloy. The effectiveness of these antiferromagnetic interlayers is due to the fact that they suppress the order parameter in the superconducting layers to a depth of $\sim\xi(T)$. The strong effect of these interlayers, however, requires that rather thick Pb-18 Å Bi layers be used in order to retain the superconductivity, and this limits the range in which these structures can be studied. In those experiments the samples were prepared by alternate deposition of the alloy and chromium, with the Pb-18 Å Bi layers deposited thermally and the chromium layers with the use of an electron gun. To decrease the effect of surface pinning, thicker, 300 Å Cr layers were deposited at the beginning and at the end of the deposition of the superconducting structure. Figure 26 shows the bulk pinning force as a function of the magnetic field in parallel and perpendicular fields. This figure shows a large anisotropy: $F_{p\parallel} \gg F_{p\perp}$.

In a perpendicular field the pinning force is governed by the interaction of the vortices with the boundaries of the granules. Calculation of the elementary pinning forces and the summation of these forces to determine the bulk pinning force are difficult in this case. The situation is considerably simplified for the calculation of these forces in a parallel field. It is known[115] that near the boundary separating the antiferromagnetic and the superconducting films the superconducting order parameter falls to zero and the thermodynamic critical magnetic field varies in this region as

$$\Delta H_c/H_c = \mathrm{th}(x/\sqrt{2}\xi) - 1, \tag{3.6}$$

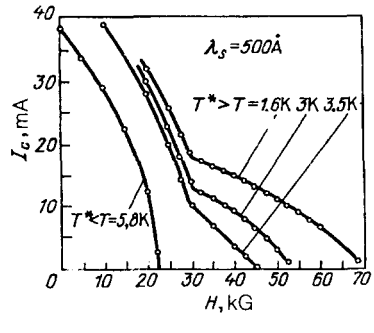

FIG. 25. Critical current as a function of the parallel magnetic field for a sample with $\lambda_s = 500$ Å (Ref. 107).

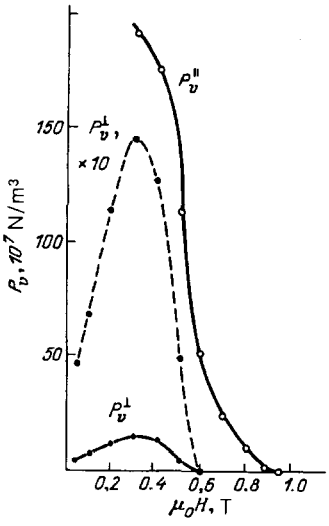

FIG. 26. Perpendicular and parallel pinning forces as functions of the magnetic field for a layered Pb–Bi/Cr sample; total sample thickness 9100 Å, 11 layers (Ref. 108).

where x is the distance from the granule. Figure 27 shows schematically an example of $\Delta H_c/H_c$ for the layered structure Cr/Pb–Bi. It follows from formula (3.6) that in the case of thin ($d \leqslant \xi$) superconducting interlayers the order parameter decreases on the average (Fig. 27b). The variation of the modulus of the order parameter in the direction of the x axis results in the generation of pinning centers. A formula was found[108] for the determination of the elementary pinning force

$$f_p \approx \frac{1}{6\sqrt{2\pi}}(1-h)H_c^2 g_1 \eta_1(g_1), \tag{3.7}$$

where g_1 is the shortest reciprocal lattice vector of the vortex lattice and η_1 is the Fourier transform of the function $(-\Delta H_c/H_c)$. It follows from formula (3.7) that $f_p \approx 200$ N/m^2, which is close to its experimental value.

Confirmation of the strong suppression of the superconducting order parameter by antiferromagnetic interlayers is another result obtained in Ref. 108. In a parallel field and for sufficiently thick superconducting layers the pinning force increased with decreasing thickness, i.e., with increasing density of pinning centers. However, at $d \approx 3\xi$ an abrupt, approximately severalfold decrease was observed, which demonstrated, in agreement with formula (3.6) and Fig. 27, the ineffectiveness of the pinning centers when they are separated by a distance less than or of the order of the coherence length.

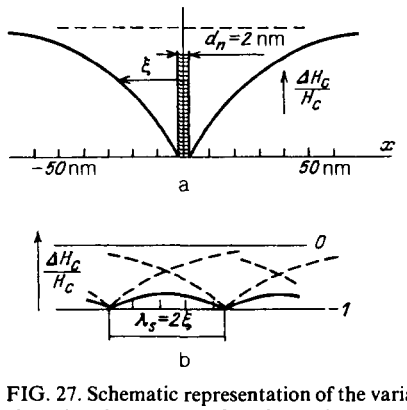

FIG. 27. Schematic representation of the variation of H_c: a) near a single chromium layer and b) for a layered structure (Ref. 108).

The layered structures of the S/s and S/I type, used in the work reported in Refs. 109–112 have important advantages from this point of view. First, these interlayers, particularly the oxides, have little effect on the order parameter in the superconducting layers. Therefore, the period of such a structure can be made very short, down to tens of angstroms. Second, in these interlayers the order parameter tends to zero, and as a consequence these interlayers must be effective vortex pinning centers. A number of interesting results have been obtained for structures of this sort. For example, Murduck *et al.*[109] have studied the layered structure NbN/AlN, prepared by dc reactive magnetron sputtering. The thickness of the insulating AlN layers was 20 Å, and that of the NbN layers was in the range from 30 to 350 Å. The samples used contained 30 layers of NbN and 31 layers of AlN. It was observed that, as in Ref. 106, the pinning force in a parallel field and the anisotropy (the ratio $I_{c\parallel}/I_{c\perp}$) increased with decreasing thickness of the superconducting layers. This means that pinning occurs at the boundaries of the layers. The critical current density for these samples in a parallel magnetic field was 10^5 A/cm^2 at $B = 21$ T.

Kadin and his coworkers[110] studied the current-carrying capacity of layered structures formed by layers of refractory metals (Nb, Mo, W) and semiconductors (Si, Ge). The structures were prepared by rf magnetron sputtering. The layer thickness for the various samples varied from a few angstroms to 50 Å, and the number of layers from 20 to 400. In these samples in a magnetic field parallel to the layers, the critical current was found to be anisotropic relative to the direction of the magnetic field. This anisotropy was observed even in the case of layers much thinner than the coherence length (one of the samples had 7 Å niobium layers and 8 Å silicon layers). Those investigators attributed the observed effect to the fact that the metal interface with the semiconductor and the semiconductor interface with the metal have different properties, which can result in a difference in the forces of interaction between the vortices and these interfaces.

Pinning in S/I layered structures has also been studied in Refs. 111 and 112. For these experiments Nb–NbO$_x$ structures were used. The niobium layers were deposited by dc magnetron sputtering to a thickness in the range 300 to 1000 Å. The oxide interlayers were formed by oxidation of the niobium layers. The results of these investigations were in agreement with the theoretical concept of two pinning mechanisms. In layered structures with a long period, where $H_{c2}(T) \gg B_{10}$, the critical current in the strong fields is determined by shear deformation in the vortex lattice. As both the period of the layer and the magnetic field strength are reduced the lattice is disrupted, the vortices enter a regime of fluid flow, and the bulk pinning force is determined by the direct summation of the elementary pinning forces in the oxide layers. Evidence for this picture comes from the way in which the bulk pinning force varies as a function of the magnetic field and of the interlayer thickness, and from the magnitude of this force. The pinning force for the case

$H_{c2}(T) \gg B_{10}$ in strong fields is close in form to $P_v(h) \sim (I-h)^2$, which is characteristic of pinning determined by shear deformation. To this situation corresponds the fact that the oxide layer interacts with only a small number of the vortices. For example, in the case of samples with $d = 900$ Å in a parallel field close to $H_{c2}^{\parallel}$ ($T = 4.2$ K), if it is assumed that the vortex lattice is thereby only slightly distorted, then only a quarter of the vortices are found to interact with the interfaces between the layers. In the case of samples with long periods, when $H_{c2}(T) \gg B_{10}$, the critical current $J_c(H)$ at low temperatures is close to that derived by Raffy *et al.*[102-104] In addition to a peak in $J_c(T)$, whose position depends mainly on the temperature, the bulk pinning force has a peak at the matching field at $B = B_{10}$. Thus, the matching effect can appear in layered structures with an effective modulation of the order parameter. Another form of behavior of the pinning force has been observed for samples with a short period, with $H_{c2}(T) \leqslant B_{10}$. In this case $P_v(h) \sim h(I-h)$, which is characteristic of the direct summation of the elementary pinning forces. It has been observed[112] that the temperature scaling behavior for these structures breaks down (Fig. 28) because the upper critical magnetic field varies with the temperature. Here, with a variation only in the temperature it is possible to go from a high density of pinning centers to the limit of a low density, a result that also explains qualitatively the change in the form of $P_v(h)$. The unimportant role of surface pinning in these structures can be explained by the irregularity of their surfaces, which makes it easy for vortices to penetrate into the interior of the sample.

In layered samples with thin superconducting interlayers it is easy to carry out the summation over the elementary pinning forces if the elastic interaction between the vortices is neglected. Assuming that the elementary pinning force is due to the change in the amplitude of the order parameter at the superconductor/insulator interface we find

$$P_v \approx (d_n H_c^2/8\phi_0) H(1-h), \tag{3.8}$$

where d_n is the thickness of the insulating interlayer. The factor $(1-h)$ in this formula comes from the decrease in the energy of condensation in a magnetic field. This form of behavior is possible if the elementary pinning forces exceed the elastic interaction between the vortices in the lattice. It was found that in accord with expression (3.8) the temperature dependence of the critical current $I_c(T)$ with h constant for samples with a short-period layered structure is close in form to $I_c(T) \sim (T_c - T)^2$, where T_c is the critical temperature of the sample.

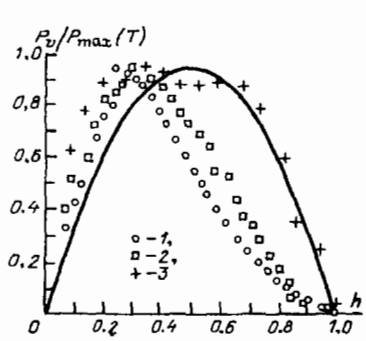

FIG. 28. Normalized dependence of the pinning force on the reduced parallel magnetic field for a Nb–NbO structure with $\lambda_s = 600$ Å. *1*—$T = 4.18$ K, $H_{c2}^{\parallel} = 18$ kOe, $P_{max} = 8.7 \cdot 10^8$ N/m^3; *2*—$T = 4.8$ K, $H_{c2}^{\parallel} = 11.4$ kOe, $P_{max} = 1.3 \cdot 10^8$ N/m^3; *3*—$T = 5.4$ K, $H_{c2}^{\parallel} = 5.5$ kOe, $P_{max} = 2 \cdot 10^7$ N/m^3. The solid line shows $P(h) \sim h(1-h)$ (Ref. 112).

3.3. Theory

The experiments of Raffy *et al.* stimulated a number of theoretical papers.[75,116,117] Among these papers the work of Ami and Maki[75] should especially be noted. There, the Ginzburg–Landau theory was used to calculate $I_c(H)$ and $P_v(H)$ for the case of matching vortex and inhomogeneity lattices. It was assumed in the calculations that the impurities affect only the diffusion coefficient D. Since the electron mean free path is inversely proportional to the concentration of inhomogeneities, Eq. (3.4) gives $D(\mathbf{r}) = D_0\{1 + \Gamma \sin[\mathbf{q}_0(\mathbf{r} - \mathbf{r}_0)]\}^{-1}$, where $|\mathbf{q}| = 2\pi/\lambda_s$, $\mathbf{r}_0 \| \mathbf{q}_0$, and $0 \leqslant |\mathbf{r}_0| \leqslant \lambda_s$. The number of layers in the sample is assumed to be infinite. The Ginzburg–Landau equations in reduced coordinates become

$$\left\{\left(\frac{\nabla}{i\varkappa_0} - \mathbf{A}\right)\frac{1}{1 + \Gamma \sin[\mathbf{q}_0(\mathbf{r} - \mathbf{r}_0)]}\left(\frac{\nabla}{i\varkappa_0} - \mathbf{A}\right) - 1 + |\psi|^2\right\}\psi = 0, \tag{3.9}$$

$$\mathbf{J} = \frac{1}{2}\frac{1}{1 + \Gamma \sin[\mathbf{q}_0(\mathbf{r} - \mathbf{r}_0)]}\left[\psi^*\left(\frac{\nabla}{i\varkappa_0} - \mathbf{A}\right)\psi + \text{c.c.}\right], \tag{3.10}$$

where $\varkappa_0$ is the Ginzburg–Landau parameter in the case $\Gamma = 0$. The solution of these equations, as usual, is sought near H_{c2}. For this purpose it is assumed that the magnetic field $\mathbf{H}$ is along the z axis. For a homogeneous superconductor, i.e., for the case $\Gamma = 0$, the solution of equations (3.9) and (3.10) is well known.[61] Qualitatively those investigators express the solution in the form of a regular triangular lattice of quantized magnetic vortices in the superconductor. As is the case for corrugated films, the matching of the vortex lattice with a lattice of inhomogeneities is possible in layered superconductors in a certain range of magnetic field near the matching field, defined by a simple geometric relation of type (2.16). Here the unit cell of the vortex lattice is already a distorted triangle (Fig. 29).

The system of Eilenberger[76] orthogonal functions (2.36) and (2.37) was used to solve the system of equations (3.9) and (3.10). The order parameter was determined by

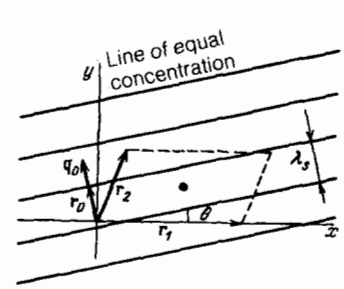

FIG. 29. Arrangement of the unit cells of the vortex lattice in a layered structure. The center of the vortex is indicated by the dark dot (Ref. 75).

the use of a linear approximation to $\Delta(\mathbf{r})$ in Eq. (3.9), that is, the last term is neglected. It is admissible to do this because the order parameter is small near H_{c2}. Moreover, it is assumed that the Eilenberger function for the vortex lattice can be written in the form (2.41). To retain only two terms in the expansion of this function is permissible if the amplitude Γ of the variation of the impurity concentration is small. When the magnetic field is changed the vortex lattice will not only be distorted but also rotated about the z axis. Below, it is assumed that one of the sides of the parallelogram forming the unit cell is always directed along the x direction and the inhomogeneity lattice rotates relative to this cell (Fig. 29). In the general case the impurity concentration varies along the vector

$$\mathbf{q}_0 = \frac{2\pi}{\lambda_s}(-\sin\theta, \cos\theta). \tag{3.11}$$

Since $\Gamma \ll 1$, the expression for the diffusion coefficient can be written as

$$D(\mathbf{r}) = \frac{D_0}{(1-\Gamma^2)^{1/2}}\{1 - 2g\sin[\mathbf{q}_0(\mathbf{r}-\mathbf{r}_0)]\}, \tag{3.12}$$

where

$$g = \Gamma[1 + (1-\Gamma^2)^{1/2}]^{-1}. \tag{3.13}$$

Solving the linearized equation (3.10) and substituting into it the Eilenberger functions of form (2.36) and (2.37), Ami and Maki determined the coefficient w_1 and the eigenvalue of this equation. Then the procedure of calculating the free energy was similar to the approach of Abrikosov.[61] The critical current, as usual, was determined from the condition of balance of two forces, the Lorentz force and the pinning force. The spatial variation of the impurity concentration plays the role of the pinning centers. In writing Eq. (3.13) it was assumed that the current flows in the plane of the layers. In this model it is assumed that when the vortex lattice and the inhomogeneity lattice do not match, the critical current through the sample goes to zero. This is a consequence of the assumption that the amplitude of the impurity concentration is small, and as a result the elastic interaction among the vortices in the lattice exceeds the elementary pinning force. With this assumption a superconducting current arises only in the region of matching of the vortex and defect lattices. In the work cited,[75] the investigators considered the special case of matching where B was near B_{n0}. In these regions of matching the free energy is given by the expression

$$F = \frac{1}{2} + B^2 - \frac{1}{1+\beta_A(2\tilde{\varkappa}_0^2-1)}\{\tilde{\varkappa}_0 - B[1 + 2gQ(B)\sin(\mathbf{q}_0\mathbf{r}_0)]\}^2, \tag{3.14}$$

where $\tilde{\varkappa}_0 Q(B)$ and β_A are defined by

$$\tilde{\varkappa}_0 = \varkappa_0(1-\Gamma^2)^{1/2}, \tag{3.15}$$

$$Q(B) = \left(1 - \frac{\pi\Phi_0}{\lambda_s^2 B}\right)\exp\left(-\frac{\pi\Phi_0}{2\lambda_s^2 B}\right), \tag{3.16}$$

$$\beta_A = n\lambda_s\frac{\varkappa_0 B}{2\pi}\sum_{p,q=-\infty}^{\infty}\cos(\pi pq)\exp\left[-n^2\lambda_s^2\frac{\varkappa_0 B}{2}(p^2+q^2)\right]. \tag{3.17}$$

It can be seen from Eq. (3.14) that the free energy varies periodically in space and direction with the period of variation of the impurity concentration. The critical current is determined by the maximum value of the pinning force due to the periodic variation in the inhomogeneity concentration. The calculations carried out in Ref. 75 show that

$$\mathbf{J}_c = \frac{\tilde{\varkappa}_0^2 q_0}{B[1+\beta_A(2\tilde{\varkappa}_0^2-1)]} \times \left\{\left[\frac{1}{16}\left(1-\frac{B}{\tilde{\varkappa}_0}\right)^2 + 2\left(\frac{B}{\tilde{\varkappa}_0}gQ(B)\right)^2\right]^{1/2} + \frac{3}{4}\left(1-\frac{B}{\tilde{\varkappa}_0}\right)\right\}^{3/2} \times \left\{\left[\frac{1}{16}\left(1-\frac{B}{\tilde{\varkappa}_0}\right)^2 + 2\left(\frac{B}{\tilde{\varkappa}_0}gQ(B)\right)^2\right]^{1/2} - \frac{1}{4}\left(1-\frac{B}{\tilde{\varkappa}_0}\right)\right\}^{1/2}\mathbf{e}_x. \tag{3.18}$$

Figure 30 shows examples of the variation of the critical current and the amplitude of the modulation of the free energy, ΔF, as functions of the external magnetic field. Reduced units are used. The parameters that characterize the sample are assumed to be the same as the experimentally determined characteristics of the samples from the experiments of Raffy *et al.*[102–104] If, as Ami and Maki did, one separates out from the experimental curves of the critical current, as a function of the magnetic field the part of the current determined only by the interaction of the vortex lattice with the layered structure, then good agreement is obtained between theory and experiment. This agreement is found not only in the shape of the curve $J_c(H)$, but also in the positions of the maxima.

M. Kulic and L. Dobrosavljevic[116] also calculated the critical current density and the pinning forces in layered superconducting structures with matched vortex and inhomogeneity lattices. Unlike the work of Ami and Maki, where the calculations were carried out for magnetic fields close to H_{c2}, in these calculations it was assumed that the magnetic field was in the range $H_{c1} \ll H \ll H_{c2}$ and that the sample had a finite thickness $D_s \gg \lambda(T)$. Although the external magnetic field is usually comparable to the upper critical field in

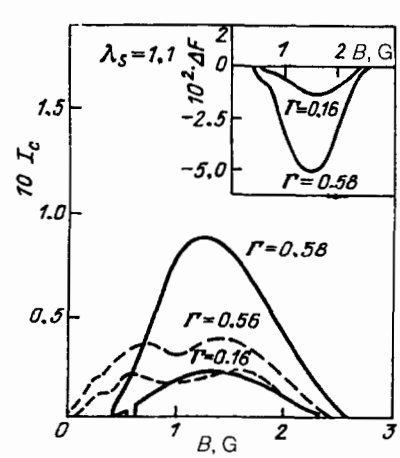

FIG. 30. Theoretical dependence of the critical current on the magnetic field. The inset shows the dependence of the amplitude of the free energy modulation on the magnetic field (Ref. 75).

experimental investigations, the work of Kulic and Dobrosavljevic[116] is of definite interest, mainly because both bulk and surface pinning were studied. They assumed that the impurity concentration in the sample varied sinusoidally according to Eq. (3.4) along the x axis with these restrictions on the period and amplitude: $\Gamma \ll 1$ and $\lambda_s \ll \lambda(T)$. The magnetic field was taken to be along the z axis, with the transport current flowing along the y axis. The vortex lattice in the x-y plane could be represented as a series of vortex chains directed along the y axis. The spacing between the nearest-neighbor vortices in any row was a_1. By means of this approach the investigators were able to use the method developed by Schmidt[118] for the investigation of the interaction between vortices and the surface of a superconductor. The free energy of the vortices in thick and homogeneous films of unit thickness and unit height can be written as

$$F = \frac{\phi_0}{8\pi a_1} \sum_l H_l. \tag{3.19}$$

To determine the free energy and the pinning force it is first necessary to find the distribution of the magnetic field in the sample. This is done with the London equation, which takes into account the spatial variation of the penetration depth of the magnetic field:

$$H_{ll'}(\mathbf{r}_l) - \lambda^2(x_l)\nabla^2 H_{ll'}(\mathbf{r}_l) - \frac{d\lambda^2(x_l)}{dx_l}\frac{\partial H_{ll'}(\mathbf{r}_l)}{\partial x_l} = \phi_0 \sum_m \delta(\mathbf{r}_l - \mathbf{r}_{l'm}), \tag{3.20}$$

where

$$\nabla^2 = \frac{\partial^2}{\partial x^2} + \frac{\partial^2}{\partial y^2},$$

$H_{ll'}(\mathbf{r}_l)$ is the magnetic field produced at the point with the coordinates $(x_l,0)$ in the x-y plane by a row of vortices intersecting the x axis at the point $x_{l'}$; here $\mathbf{r}_l = (x_l,0)$ and $\mathbf{r}_{l'm} = (x_{l'},ma_1)$, with $m = 0,1,2,\ldots$. This approach is valid for superconductors with a large Ginzburg–Landau parameter. Since λ^2 is proportional to the concentration,

$$\lambda^2(x) = \lambda_0\left(1 + \Gamma\cos\frac{2\pi x}{\lambda_s}\right).$$

In this case $\varkappa$ also varies in space: in the region of the maximum concentration $\varkappa = \varkappa_0(1+\Gamma)$. Equation (3.20) is solved by means of a Fourier transformation. After determining the magnetic field, the authors of Ref. 116 calculated the Gibbs free energy; then minimizing it, they were able to find the equilibrium vortex lattice in the layered structures, and then using the usual relation (2.49) for the pinning found the dependence of the critical current on the magnetic field near the matching field B_{10}

$$J_c = \frac{c\lambda_s}{8\pi D_s\lambda_0}\left[[(H-B) + \frac{\Gamma}{\pi}(2H+B)] + 2\Gamma\frac{D_s}{\lambda}\left\{\frac{B}{\pi} - \frac{\Phi_0}{\lambda_s^2}\left[\ln(1-e^{-B\tilde{\lambda}}) + \frac{e^{-B\tilde{\lambda}}}{1+(\tilde{B}\tilde{\lambda})^2(\varkappa_0\tilde{\lambda}/\pi)^2}\right]\right\}\right], \tag{3.21}$$

where $\tilde{B} = B/\sqrt{2}H_c$ and $\tilde{\lambda} = \lambda_s/\lambda_0$.

The first term in (3.21) corresponds to the interaction of the vortices with the surface of the semiconductor, and is inversely proportional to the thickness of the sample. The second term in this expression comes from the volume interaction of the vortex lattice with the lattice of inhomogeneities. This term does not depend on the sample thickness, and is proportional to the amplitude of the variation of the impurity concentration. As shown in Eq. (3.21), the relation between these pinning mechanisms depends on the quantity $\Gamma D_s/\lambda_0$. In the case of a thick film with a rather large modulation amplitude, where $\Gamma_s/\lambda_0 \gg 1$, surface pinning can be neglected, and conversely, when $\Gamma D_s/\lambda_0 \approx 1$ surface pinning is as important as bulk pinning.

One of the main shortcomings of the work of Refs. 75 and 116 is that it does not allow for the dependence of the pinning force on the magnetic field and the dimensions of the sample. Besides the approach developed in these papers, which is based on the Ginzburg–Landau equations, a completely different method[117] can be used to calculate pinning in layered structures. This method takes into account the elastic properties of the vortex lattice, and it makes up for the shortcomings noted above concerning the calculations of Ref. 75 and 116. Lowell[117] has considered the vortex lattice as a one-dimensional elastic continuum. Its behavior, when the Lorentz force is constant in space and is directed, as usual, along the x axis, is governed by the balance between the elastic and pinning forces. When the pinning force is smaller than the elastic interaction ($f_p \ll \mu a_1$) the equation is

$$\mu\frac{d^2x_1}{dx^2} = \frac{f_p}{a_1}\sin\frac{2\pi x}{\lambda_s}, \tag{3.22}$$

where x is the coordinate of the nth vortex, a_1 is the distance between the vortices in a chain, and $x_1(x)$ is the displacement of a vortex from its equilibrium position. Since x_1 and x are related by $x = na_1 + x_1$, Eqs. (3.22) can be written as

$$\frac{d^2x_2}{dx^2} = \frac{f_p\lambda_s}{\mu a_1^2}\sin\frac{2\pi x_2}{\lambda_s}, \tag{3.23}$$

where the following notation is introduced:

$$x_2(x) = \frac{a_1 - \lambda_s}{a_1}x + \frac{\lambda_s}{a_1}x_1.$$

Equation (3.23) is readily solved,[117] and with the appropriate boundary conditions the solution gives the dependence $x_2(x)$. As a result the net pinning force F_p is obtained by integration

$$F_p = \int_0^{D_s}\frac{f_p}{a_1}\sin\frac{2\pi x_2}{\lambda_s}dx = \frac{2pf_p}{\lambda_s m^{1/2}}\left[dn\left(z - \frac{D_s}{pm^{1/2}}\middle|m\right) - dn\left(z + \frac{D_s}{2pm}\middle|m\right)\right]; \tag{3.24}$$

where $\mathrm{dn}(u|m)$ is the function defined by Milne–Thompson,[119]

$$z = (x'/pm^{1/2}) + (D_s/2pm^{1/2}),$$
$$m = (2\pi f_p/\mu a_1^2)x_0^2 = x_0^2/p^2;$$

and x_0 and x_1 are constants specified by the boundary conditions.

Using this approach, Lowell[117] obtained two important results. The first was for the case of matching vortex and inhomogeneity lattices ($a_1 = \lambda_s$), where he found the dependence of the pinning force on the sample thickness (Fig. 31). For thin samples ($D_s \lesssim p$) the pinning force is close in form to Nf_p (N is the number of layers), that is, close to the pinning force that arises when each vortex interacts synchronously with the inhomogeneities in the superconductors. For thick samples, ($D_s \gtrsim p$) the pinning force is approximately $F_p = 4Nf_p/D_s$, that is, in this limit the total pinning force does not depend on the sample thickness, and another rule must be used for summing the elementary pinning forces: $F_p \sim f_p^{1/2}$. The results obtained by Lowell are in agreement with previous model calculations[119] based on the approaches described in the monograph of Campbell and Evetts.[101] The second important result of the work of Lowell is the calculated magnetic-field dependence of the pinning forces over a wide range of magnetic field. This dependence was calculated in two important limits: $D_s \ll p$ and $D_s \gg p$, i.e., for the two cases of a small and a large number of layers. Figure 32 shows examples of this dependence of the resultant pinning force on the magnetic field. In accordance with Fig. 31, for $D_s/p = 0.3$, it was assumed that $F_0 = f_p D_s/\lambda_s$, and for the curves $D_s/p = 5$ and 10, $F_0 = 4f_p p/\lambda_s$. In that paper it was also observed that the peak of the critical current as a function of the magnetic field in the region of matching of the periods of the vortex chain and the layered structure is much narrower than in the experiments of Raffy *et al.*[102-104] I believe that a probable cause of this phenomenon is the low rigidity of the vortex lattice as compared with the elementary pinning force. Because the bulk modulus of the vortex lattice is finite in layered superconductors unlike in thin films, it is important to investigate the effect of the self-magnetic field of the transport current on the calculated dependences. In the theoretical papers mentioned in this review it has been assumed that this field is much smaller than the external magnetic field.

After the discovery of high-T_c superconductors, which ordinarily are naturally layered structures, the study of the

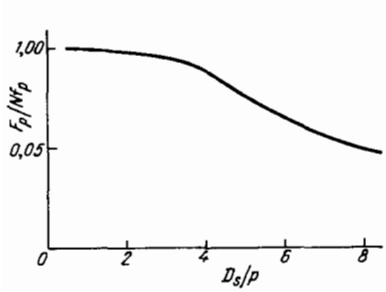

FIG. 31. Total pinning force as a function of the number of pinning centers in a chain for matching vortex and inhomogeneity lattices (Ref. 117).

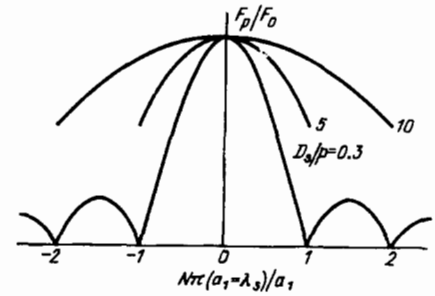

FIG. 32. Pinning force as a function of the magnetic field for various values of the parameter D_s/p (Ref. 117).

mixed state in these materials became a matter of interest. It was observed that a periodic structure of the mixed state was formed also in the direction of the external magnetic field in layered superconductors with weak coupling between the layers ($\xi_z \gg \lambda_s$), i.e., S/I superconductors. This structure, which consists of sharp periodic bends in the vortex lines, is formed in a magnetic field $H_{c1} \ll H \ll H_{c2}$ at an angle to the layers.[121] Qualitatively, the nature of its formation can be understood by the following considerations. When the magnetic field is parallel to the layers, the vortex centers, tending to minimize the free energy, must be located between the superconducting layers. This condition leads to the formation of periodic bends in the vortices in an inclined magnetic field. The extra energy of such a bend is given by

$$\varepsilon_k = \frac{\phi_0^2 d}{(4\pi\lambda_{xy})^2} \ln\frac{\lambda_s}{\xi_z}. \tag{3.25}$$

As a consequence, the formation of the bends results in a jump in the dependence of the torque on the angle in a small, nearly zero field. This phenomenon was observed experimentally in studies of high-T_c superconductors in Ref. 122.

3.4. The prospects of layered superconducting structures

First off all it should be noted that from the point of view of understanding the nature and mechanisms of pinning it is very important to study the mixed state in layered structures. For example, in these superconductors it is possible, as mentioned above, to determine the elementary pinning forces. This topic is also important. For example, even in such theoretically and experimentally well-studied structures as the S/N structures, the mechanism of elementary pinning is still unclear. In addition to such an obvious mechanism as pinning due to the suppression of the order parameter in the normal-metal interlayers by the proximity effect, it has been shown[123] that it is also important to take into account the reflection of electrons at the layer boundaries. Even in the case of thin layers of normal metal, where pinning due to suppression of the order parameter is small, the second pinning mechanism remains important.

Layered structures are also interesting from the point of view of making superconductors with higher critical currents, since non-superconducting interlayers can be effective pinning centers, and making them with higher critical magnetic fields in the direction parallel to the layers. I believe that layered structures based on thin perforated superconducting films are also of particular interest in this context.

Here, the period of the layered structure and the period of the hole lattice must be comparable with the coherence length. In these structures the holes, being effective pinning centers as is the case with single-layer films, must, as noted in Section 2.6, increase the upper critical field in the direction perpendicular to the layers; that is, in these structures one can expect an increase over ordinary bulk superconductors in the upper critical field and in the critical current.

In conclusion, I would like to discuss the possibility of using layered structures in superconducting electronics.[83] This idea is based on the fact that the period of the layered structures can be very small, down to a few angstroms. This opens up additional possibilities for the creation of new superconducting elements, including elements whose principle of operation is based on the motion of vortices. It is obvious that in short and in narrow microbridges made of layered superconducting films placed in a parallel magnetic field, a voltage is induced because of the motion of a single chain of vortices. At the contact there should arise an alternating voltage with a frequency $f_0 = e(V)/\pi\hbar$. To increase the generated power one can exploit the usual idea—use contacts in series in a chain for the alternating component of the voltage and in parallel for the dc components. Figure 33 shows a possible design for the connection of such bridge contacts. The inductances allow the contacts to be connected in parallel for dc and in series for ac. The equality of the constant voltage on the contacts guarantees equality of the generated frequency. The required phase matching of the radiation generated by the different contacts is provided in this case by a mechanism specific to vortices: by the magnetic pairing of the vortices in the superconductors separated by the insulating layer.[124] By varying the magnetic field strength, one can shift one vortex chain relative to another and thereby adjust the phase of the generated radiation. This idea is of particular interest for high-T_c superconductors, which, as is well known are natural layered superconductors, with interlayer distances of the order of several tens of angstroms. Moreover, in growing the films it is usually the case that the layers lie in the plane of the substrate. Thus, by using single-crystal high-T_c superconductor films it is possible by ordinarily lithography to make a structure like the one shown in Fig. 33. The small period of the layered structure should make it possible to increase the upper limit of the frequency of the radiation generated by the vortex lattice as it moves in a field with a periodic potential.

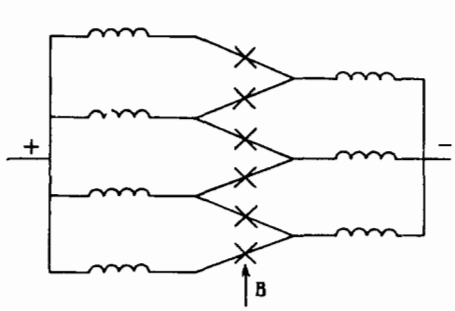

FIG. 33. Method of connecting bridge contacts made of layered structures (Ref. 83).

CONCLUSIONS

The use of ordered microstructures provides new, even quantitative, information on the elementary pinning forces and gives rise to interesting effects based on the coherent behavior of the Abrikosov vortices in them. A great deal of progress has been made in these fields. I believe that at the present time a very important problem is the study of quasi-periodic structures and the pinning that occurs in them. The reason for this opinion is that such structures are intermediate between a completely ordered superconducting lattice and a random system of pinning centers, which exists in ordinary superconductors. One of the principal goals of the present review was to call attention to this problem, and to show that there are interesting problems both from the fundamental and the applied point of view. It should also be mentioned that the rapid development of technology gives grounds to anticipate that shortly it will be possible to make more complicated and more perfect superconducting microstructures. This dynamism also indicates the immediate importance of this field of research.

In conclusion, I would like to express my sincere gratitude to A. A. Abrikosov for his attention to this work and his constant advice at various stages of this work, and also to V. V. Kuziĭ for fruitful discussions.

[1] V. L. Ginzburg and L. D. Landau, Zh. Eksp. Teor. Fiz. **20**, 1064 (1950).
[2] T. R. Dinger, T. K. Worthington, W. J. Gallagher, and R. L. Sandstrom, Phys. Rev. Lett. **58**, 2687 (1987).
[3] L. Solymar, *Superconductive Tunneling and its Applications*, Chapman and Hall, London (1972).
[4] K. K. Likharev and B. T. Ul'rikh, *Systems with Josephson Junctions*, Moscow State University (1978).
[5] L. G. Aslamazov and A. I. Larkin, Pis'ma Zh. Eksp. Teor. Fiz. **9**, 150 (1969) [JETP Lett. **9**, 87 (1969)].
[6] L. G. Aslamazov and A. I. Larkin, Zh. Eksp. Teor. Fiz. **74**, 2184 (1978) [Sov. Phys. JETP **47**, 1136 (1978)].
[7] S. N. Artemenko, A. F. Volkov, and A. V. Zaitsev, Zh. Eksp. Teor. Fiz. **76**, 1816 (1979) [Sov. Phys. JETP **49**, 924 (1979)].
[8] A. V. Zaĭtsev, Zh. Eksp. Teor. Fiz. **78**, 221 (1980) [Sov. Phys. JETP **51**, 111 (1980)].
[9] T. M. Klapwijk, G. E. Blonder, and M. R. Tinkham, Physica B + C **109–110**, 1657 (1982).
[10] M. Octavio, M. R. Tinkham, T. M. Klapwijk, and G. E. Blonder, Phys. Rev. B **27**, 6739 (1983).
[11] W. J. Skocpol, M. R. Beasley, and M. Tinkham, J. Low Temp. Phys. **16**, 145 (1974).
[12] W. J. Skocpol, Phys. Rev. B **14**, 1045 (1976).
[13] P. W. Anderson and A. H. Dayem, Phys. Rev. Lett. **13**, 195 (1964).
[14] V. N. Gubankov, V. P. Koshelets, K. K. Likharev, and G. N. Ovsyannikov, Pis'ma Zh. Eksp. Teor. Fiz. **18**, 292 (1973) [JETP Lett. **18**, 171 (1973)].
[15] K. K. Likharev and L. A. Yakobson, Zh. Tekh. Fiz. **45**, 1503 (1975) [Sov. Phys. Tech. Phys. **20**, 950 (1975)].
[16] M. Yu. Kupriyanov, K. K. Likharev, and L. A. Maslova, *Proc. 14th Intern. Conf. on Low Temperature Physics*, Helsinki (1975), Vol. 4, p. 104.
[17] K. K. Likharev, Rev. Mod. Phys. **51**, 101 (1979) [Earlier version in Russian in Usp. Fiz. Nauk **127**, 185 (1979)].
[18] V. N. Gubankov, V. P. Koshelets, and G. N. Ovsyannikov, Zh. Eksp. Teor. Fiz. **71**, 348 (1976) [Sov. Phys. JETP **44**, 181 (1976)].
[19] S. Benacka, L. Bezakova, S. Gazi, and S. Takacs, Czech J. Phys. B **28**, 203 (1978).
[20] H. A. Notarys, R. H. Wang, and J. E. Mercereau, Proc. IEEE **61**, 79 (1973).
[21] R. B. Laibowitz, Appl. Phys. Lett. **23**, 407 (1973).
[22] P. Crozat, S. Gourrier, D. Bouchon, and G. Adde, *Proc. 14th Intern. Conf. on Low Temperature Physics*, Helsinki (1975), Vol. 4, p. 206.
[23] K. K. Likharev, Zh. Eksp. Teor. Fiz. **61**, 1700 (1971) [Sov. Phys. JETP **34**, 906 (1971)].

[24] L. G. Aslamazov and A. I. Larkin, Zh. Eksp. Teor. Fiz. **68**, 766 (1975) [Sov. Phys. JETP **41**, 391 (1975)].
[25] L. P. Gorkov and N. B. Kopnin, Zh. Eksp. Teor. Fiz. **60**, 2331 (1971) [Sov. Phys. JETP **33**, 1251 (1971)].
[26] P. Crozat, G. Vernet, and G. Adde, *Proc. Second Intern. Conf. SQUID-80. Superconducting Quantum Interference Devices and Their Applications*, Berlin, Walter de Gruyter, New York, (1980), p. 157.
[27] R. Gross, H. Seifert, R. P. Huebener, and K. Yoshida, J. Low Temp. Phys. **54**, 277 (1984).
[28] D. W. Palmer, H. A. Notarys, and J. E. Mercereau, Appl. Phys. Lett. **25**, 527 (1974).
[29] M. A. Janocko, J. R. Gavaler, C. K. Jones, and R. D. Blaugher, J. Appl. Phys. **42**, 182 (1971).
[30] J. H. Claassen, E. J. Cukauskas, and M. Niseoff, *Proc. Second Intern. Conf. SQUID-80. Superconducting Quantum Interference Devices and their Applications*, Berlin, Walter de Gruyter, New York (1980), p. 333.
[31] C. T. Wu and C. M. Falko, Appl. Phys. Lett. **30**, 609 (1977).
[32] T. W. Lee and C. M. Falco, IEEE Trans. Magn. **MAG-17**, 85 (1981).
[33] A. I. Golovashkin, I. S. Levchenko, A. N. Lykov, and L. I. Makhashvili, Pis'ma Zh. Eksp. Teor. Fiz. **24**, 565 (1976) [JETP Lett. **24**, 521 (1976)].
[34] A. I. Golovashkin and A. N. Lykov, Zh. Eksp. Teor. Fiz. **74**, 214 (1978) [Sov. Phys. JETP **47**, 110 (1978)].
[35] A. I. Golovashkin and A. N. Lykov, and S. L. Prishchena Zh. Eksp. Teor. Fiz. **76**, 1316 (1979) [Sov. Phys. JETP **49**, 668 (1979)].
[36] S. Kuriki, A. Yoshida, and H. Konishi, J. Low Temp. Phys. **51**, 149 (1983).
[37] C. E. Gough, M. S. Colclough, E. M. Forgan, B. G. Jordan, M. Keene, C. M. Muirhead, A. I. M. Rae, N. Thomas, J. S. Abell, and S. Sutton, Nature **326**, 855 (1987).
[38] I. Igichi, A. Sugishita, and M. Yanagisawa, Jpn. J. Appl. Phys. **26**, L1021 (1987).
[39] X. F. Meng, Y. D. Dai, H. M. Jiang, X. M. Ren, Y. Zhang, M. X. Yan, Y. C. Du, J. C. Mao, S. W. Wu and G. J. Cui, Solid State Commun. **63**, 853 (1987).
[40] R. H. Koch, C. P. Umbach, G. J. Clark, P. Chaudhari, and R. B. Laibowitz, Appl. Phys. Lett. **51**, 200 (1987).
[41] G. J. Cui, X. F. Meng, S. G. Wang, K. Shao, H. M. Jiang, Y. D. Dai, Y. Zhang, R. P. Peng, Z. L. Bao, F. R. Wang, S. Z. Wang, Z. Y. Ye, C. Y. Li, K. Wu, and D. L. Yin, Solid State Commun. **64**, 321 (1987).
[42] É. M. Rudenko, I. V. Korotash, I. P. Nevirkovets, Yu. M. Boguslavskii, P. A. Zhukov, and A. G. Sivakov, Sverkphorovodimost' (KIAE) **4**, 1153 (1991) [Superconductivity **4**, 1061 (1991)].
[43] M. Yu. Kupriyanov and K. K. Likharev, Usp. Fiz. Nauk **160**, 49 (1990) [Sov. Phys. Usp. **33**, 340 (1990)].
[44] M. R. Beasley, "Improved Materials for Superconducting Electronics," AIP Conf. Proc. **44**, 389 (1978).
[45] A. N. Lykov, Fiz. Tverd. Tela (Leningrad) **24**, 3353 (1982) [Sov. Phys. Solid State **24**, 1905 (1982)].
[46] M. R. Beasley, R. Labush, and W. W. Webb, Phys. Rev. **181**, 682 (1969).
[47] Y. Yeshurun and A. P. Malozemoff, Phys. Rev. Lett. **60**, 2202 (1988).
[48] P. W. Anderson, Phys. Rev. Lett. **9**, 309 (1962).
[49] A. N. Lykov and S. L. Prishchena, Fiz. Tverd. Tela (Leningrad) **26**, 961 (1984) [Sov. Phys. Solid State **26**, 587 (1984)].
[50] A. I. Golovashkin, A. N. Lykov, and S. L. Prishchena, Krat. Soobshch. Fiz. FIAN [P. N. Lebedev Physics Institute] No. 12, 45 (1983)].
[51] G. Deutscher, Y. Imry, and L. Gunther, Phys. Rev. B **10**, 4598 (1974).
[52] J. R. Clem, B. Bumble, S. I. Raider, W. J. Gallagher, and Y. C. Shih, Phys. Rev. B **35**, 6637 (1987).
[53] B. J. Orr, J. R. Clem, H. M. Jaeger, and A. M. Goldman, Phys. Rev. B **34**, 3491 (1986).
[54] B. Hauser, B. B. G. Klopman, G. J. Gerritsma, J. Gao, and H. Rogalla, Appl. Phys. Lett. **54**, 1368 (1989).
[55] T. Yamashita, A. Kawakami, S. Noge, W. Xu, M. Takado, T. Komatsu, and K. Matusita, Jpn. J. Appl. Phys. **27**, L1107 (1988).
[56] D. G. Emel'yankov, U. N. Inkin, V. A. Kulikov, V. N. Laptev, L. V. Matveev, V. I. Makhov, and A. Yu. Serebryakov, Pis'ma Zh. Tekh. Fiz. **15**(21), 40 (1989) [Sov. Tech. Phys. Lett. **15**, 947 (1989)].
[57] M. A. Gijs and R. J. E. Jansen, Appl. Phys. Lett. **56**, 1484 (1990).
[58] J. Pearl, Appl. Phys. Lett. **5**, 65 (1964).
[59] M. Tinkham, Phys. Rev. **129**, 2413 (1963).
[60] K. Maki, Ann. Phys. (NY) **34**, 363 (1965).
[61] A. A. Abrikosov, Zh. Eksp. Teor. Fiz. **32**, 1442 (1957) [Sov. Phys. JETP **5**, 1174 (1957)].
[62] A. L. Fetter and P. C. Honenberg, Phys. Rev. **159**, 330 (1967).
[63] A. T. Fiory, Phys. Rev. B **8**, 5039 (1967).
[64] K. K. Efetov, Fiz. Tverd. Tela (Leningrad) **15**, 647 (1973) [Sov. Phys. Solid State **15**, 459 (1973)].
[65] V. V. Kuzii, Fiz. Nizk. Temp. **8**, 180 (1982) [Sov. J. Low Temp. Phys. **8**, 89 (1982)].
[66] D. S. Fisher, Phys. Rev. B **22**, 1190 (1980).
[67] D. D. Morrison and R. M. Rose, Phys. Rev. Lett. **25**, 356 (1970).
[68] O. Dalkini, P. Martinoli, J. L. Olsen and G. Berner, Phys. Rev. Lett. **432**, 218 (1974).
[69] P. Martinoli, O. Daldini, C. Leemann, and E. Stocker, Solid State Commun. **17**, 205 (1975).
[70] P. Martinoli, O. Daldini, C. Leemann, and B. van der Brandt, Phys. Rev. Lett. **36**, 382 (1976).
[71] P. Martinoli, Phys. Rev. B **17**, 1175 (1978).
[72] P. Martinoli, M. Nsabimana, G. A. Rasine, H. Beck, and J. R. Clem, Helv. Phys. Acta **55**, 655 (1982).
[73] X.-M. Tang, G. A. Rasine, C. Leemann, and P. Martinoli, *Proc. 18th Intern. Conf. on Low Temperature Physics*, Jpn. J. Appl. Phys. **26**, 1497 (1987).
[74] Z. Radovic, L. Dobrosavljevic, and M. Kulic, Solid State Commun. **26**, 119 (1978).
[75] S. Ami and K. Maki, Prog. Theor. Phys. **53**, 1 (1974).
[76] G. Eilengberger, Phys. Rev. **164**, 628 (1967).
[77] V. L. Prokrovskii and A. L. Talapov, Zh. Eksp. Teor. Fiz. **78**, 269 (1980) [Sov. Phys. JETP **51**, 134 (1980)].
[78] C. E. Burkov and V. L. Pokrovskii, Pis'ma Zh. Eksp. Teor. Fiz. **32**, 285 (1980) [JETP Lett. **32**, 263 (1980)].
[79] A. Pruijboom, E. van der Druft, and P. H. Kes, Physica C **165**, 179 (1990).
[80] A. I. Larkin and Yu. N. Ovchinnikov, J. Low Temp. Phys. **34**, 409 (1979).
[81] A. I. Larkin and Yu. N. Ovchinnikov, in *Nonequilibrium Superconductivity*, E. Langeberg and A. I. Larkin (eds.) North-Holland, Amsterdam, (1986), p. 493.
[82] A. N. Lykov, V. B. Mukhachev, and A. D. Krivospitskii, Fiz. Nizk. Temp. **14**, 130 (1988) [Sov. J. Low Temp. Phys. **14**, 71 (1988)].
[83] A. N. Lykov, Pis'ma Zh. Tekh. Fiz. **11**, 331 (1985) [Sov. Tech. Phys. Lett. **11**, 135 (1985)].
[84] A. T. Fiory, A. F. Hebard, and S. Somekh, Appl. Phys. Lett. **32**, 73 (1978).
[85] J. R. Clem, Phys. Rev. B **9**, 898 (1974).
[86] M. G. Blamire, J. Low Temp. Phys. **68**, 335 (1987).
[87] M. G. Blamire and J. E. Evets, Philos. Mag. B **51**, 421 (1985).
[88] H. M. Miesenböck, J. Low Temp. Phys. **56**, 1 (1984).
[89] A. D. Krivospitski and A. N. Lykov, Pis'ma Zh. Tekh. Fiz. **15**(21), 37 (1989) [Sov. Phys. Lett. **15**, 845 (1989)].
[90] A. N. Lykov, Solid State Commun. **85** (1992).
[91] B. Pannetier, J. Chaussy, and R. Ramal, J. Phys. (Paris) Lett. **44**, L853 (1983).
[92] W. Bächtold, IEEE Trans. Magn. MAG-15, 558 (1979).
[93] A. F. Hebard and A. T. Fiory, *A Memory Device Utilizing the Storage of Abrikosov Vortices*, AIP Conf. Proc. **44**, 465 (1978).
[94] B. Y. Jin and J. B. Ketterson, Adv. Phys. **38**, 189 (1989).
[95] R. A. Klemm, M. R. Beasley, and A. Luther, J. Low Temp. Phys. **16**, 607 (1974).
[96] T. M. Rice, Phys. Rev. **140A**, 1889 (1965).
[97] I. E. Dzyaloshinskii and E. I. Kats, Zh. Eksp. Teor. Fiz. **55**, 2373 (1968) [Sov. Phys. JETP **28**, 1259 (1969)].
[98] J. Friedel, J. Phys. Cond. Matter **1**, 7757 (1989).
[99] S. E. Korshunov, Europhys. Lett. **11**, 757 (1990).
[100] B. Horovitz, Phys. Rev. Lett. **67**, 378 (1991).
[101] A. M. Campbell and J. E. Evetts, Adv. Phys. **21**, 199 (1972).
[102] H. Raffy, J. C. Renard, and E. Guyon, Solid State Commun. **11**, 1679 (1972).
[103] H. Raffy, J. C. Renard, and E. Guyon, Solid State Commun. **14**, 427 (1974).
[104] H. Raffy, J. C. Renard, and E. Guyon, Solid State Commun. **14**, 431 (1974).
[105] P. R. Broussard and T. H. Geballe, Phys. Rev. B 37, **68** (1988).
[106] A. J. Vermeer, C. W. Hagen, D. G. de Groot, N. J. Koeman, J. H. Rector, H. van Leuken and R. Griessen, *Proc. Intern. Conf. on Materials and Mechanisms of Superconductivity. High Temperature Superconductors II* (California). Physica C **162–164**, 409 (1989).
[107] L. Antognazza, M. G. Karkut, J.-M. Triscone, V. Matijasevic, N. Missert, M. R. Beasley, and O. Fischer, *Proc. Intern. Conf. on Materials and Mechanisms of Superconductivity. High Temperature Superconductors II* (California). Physica C **162–164**, 411 (1989).
[108] W. E. Yetter, E. J. Kramet and D. G. Ast, J. Low Temp. Phys. **49**, 227 (1982).
[109] J. M. Murduk, D. W. Capone, I. K. Schuller, S. Foner, and J. B. Ketterson, Appl. Phys. Lett. **52**, 504 (1988).
[110] A. M. Kadin, R. W. Burkhardt, J. T. Chen, J. E. Keem, and S. R. Ovshinsky, *Proc. 17th Intern. Conf. on Low Temperature Physics*, U. Echer, A. Schmidt, W. Weber, and H. Wulf (Eds.), North Holland, Amsterdam (1984), p. C09.
[111] V. I. Dedyu, A. N. Lykov, and S. L. Prishchena, Zh. Eksp. Teor. Fiz. **97**, 872 (1990) [Sov. Phys. JETP **70**, 488 (1990)].

[112] A. N. Lykov and V. I. Zdrevkov, Pis'ma Zh. Tekh. Fiz. **17**(8), 73 (1991) [Sov. Tech. Phys. Lett. **17**, 306 (1991)].
[113] S. Takahashi and M. Tachiki, Phys. Rev. B **34**, 3162 (1986).
[114] M. G. Karkut, V. Matijasevic, L. Antognazza, J.-M. Tiscone, N. Missert, M. R. Beasley, and O. Fischer, Phys. Rev. Lett. **60**, 1751 (1988).
[115] P. De Gennes, *Superconductivity of Metals and Alloys*, Benjamin, New York (1966).
[116] M. Kulic and L. Dobrosavljevic Phys. Stat. Solidi B **75**, 677 (1976).
[117] J. Lowell, J. Phys. F **8**, 501 (1978).
[118] V. V. Shmidt, Zh. Eksp. Teor. Fiz. **61**, 198 (1971) [Sov. Phys. JETP **34**, 211 (1971)].
[119] L. M. Milne-Thompson, Jacobian Elliptical Function Table, Dover, N. Y., 1950.
[120] J. R. Appleyard, J. E. Evetts, and A. M. Campbell, Solid State Commun. **14**, 567 (1974).
[121] B. I. Ivlev, Yu. N. Ovchinnikov, and V. L. Pokrovsky, Europhys. Lett. **13**, 187 (1990).
[122] T. R. Chien, Z. Z. Wang, and N. P. Ong, *Proc. Intern. Conf. on Materials and Mechanisms of Superconductivity. High Temperature Superconductors II* (California). Physica C **162–164**, 343 (1989).
[123] W. E. Yetter, D. A. Thomas, and E. J. Kramer, Philos. Mag. B **46**, 523 (1982).
[124] I. Giaver, Phys. Rev. Lett. **15**, 825 (1985).

Translated by J. R. Anderson